UNIVERSITY OF CALIFORNIA,
IRVINE

Ecosystem Resilience to Global Environmental Change

DISSERTATION

submitted in partial satisfaction of the requirements
for the degree of

DOCTOR OF PHILOSOPHY

in Earth System Science

by

Nicole Marie Fiore

Dissertation Committee:
Professor Michael Goulden, Chair
Associate Professor Claudia Czimczik
Professor Steven Allison

2022

Chapter 4 © 2020 Nicole Marie Fiore
All other materials © 2022 Nicole Marie Fiore

TABLE OF CONTENTS

	Page
LIST OF FIGURES	iii
ACKNOWLEDGEMENTS	v
VITA	vi
ABSTRACT OF THE DISSERTATION	ix
CHAPTER 1: Introduction	1
CHAPTER 2: Drivers and implications of a stable shrubland grassland boundary in Southern California	8
CHAPTER 3: Drought induced vegetation shifts from shrub to grassland impact above- and belowground properties	35
CHAPTER 4: Do recent NDVI trends demonstrate boreal forest decline in Alaska?	63
CHAPTER 5: Future research directions	83
APPENDIX A: Supplemental Figures	85
APPENDIX B: Supplemental Tables	88

LIST OF FIGURES

		Page
Figure 2.1	Aerial photos of the study site	16
Figure 2.2	Average species composition and percent of vegetation cover and ground cover	17
Figure 2.3	Average above and belowground live biomass and litter pools by type	18
Figure 2.4	Root properties	19
Figure 2.5	Soil texture as fractional composition of sand, silt, and clay	20
Figure 2.6	Soil properties	22
Figure 2.7	Total soil organic carbon and nitrogen stocks	23
Figure 2.8	Root structures found in 0-10 cm depth range	24
Figure 3.1	Study site and experimental design	39
Figure 3.2	Water input and cumulative water input by year and treatment	40
Figure 3.3	Live biomass and litter mass pools in Coastal Sage Scrub	44
Figure 3.4	Root biomass, soil organic carbon, and soil nitrogen stocks in Coastal Sage Scrub	45
Figure 3.5	Soil properties by depth in Coastal Sage Scrub	46
Figure 3.6	Correlation between aboveground grass litter mass and surface soil bulk density in Coastal Sage Scrub	47
Figure 3.7	Correlations between root biomass and soil organic carbon content in 0-10 and 10-20 cm in Coastal Sage Scrub	48
Figure 3.8	Correlations between root biomass and soil organic carbon content in 0-10 and 10-20 cm in Coastal Sage Scrub	50
Figure 4.1	Map of site locations	67
Figure 4.2	Boxplots of all 1999–2018 NDVI trends	70
Figure 4.3	Chronosequences of composition (based on percent cover) of upper and lower canopies, and ground cover	71

Figure 4.4 Fire history polygons overlaid on map of NDVI linear regression trends from 1999–2018 72

Figure 4.5 Chronosequences of NDVI of all sites visited, separated by dominant vegetation in the upper canopy during 2017–2018 74

Figure 4.6 NDVI trend during 1999–2018 as a function of year of fire 75

Figure 4.7 Relationships between fraction deciduous and NDVI, and LAI and NDVI 76

ACKNOWLEDGEMENTS

First and foremost, I would like to thank my advisor, Dr. Michael Goulden. Thank you for taking me on as a graduate student back in 2016, and for allowing me the freedom to explore my research interests at Loma Ridge. The breadth of your knowledge of terrestrial ecosystems is quite impressive and has helped shape how I think about ecosystem processes.

I would also like to express my appreciation for my committee members, Dr. Claudia Czimczik and Dr. Steven Allison. To Dr. Claudia Czimczik, thank you for sparking my interest in soils, and for your advice, mentorship, and friendship throughout my time at UCI. I would gladly accept any opportunity to work with you again, even if it means returning to Finger Mountain in the freezing rain. To Dr. Steven Allison, thank you for your advice and guidance in research, as well as in Ridge to Reef. I admire your dedication to climate change action, and the steps you are taking to train the next generation of scientists.

In addition, the work presented in this dissertation would not have been possible without the help of the numerous undergraduate interns who assisted in the field and the lab. Thank you, Malissa, Mel, Bianca, Eli, Jem, Alex, Connor, Quinn, David, Sara, Nervana, and Christabel.

I would like to acknowledge the funding sources that supported this dissertation. The work in Chapters 2 and 3 was funded by the United States Department of Energy's Terrestrial Ecosystem Science Program. The work in Chapter 4 was funded by NASA ABoVE (NNX15AU16A). This dissertation was also supported by the Ridge to Reef NSF Research Traineeship (DGE-1735040). A special thank you to the Irvine Ranch Conservancy for hosting the LRGCE.

Chapter 4 is reprinted from a publication in *Environmental Research Letters*, with permission from IOP Publishing.

VITA

Nicole Marie Fiore

EDUCATION

Ph.D., University of California Irvine, 2022
Earth System Science

M.S., University of California Irvine, 2019
Earth System Science

B.A., University of California Santa Cruz, 2013
Environmental Studies and Biology

RESEARCH INTERESTS

Terrestrial ecology and biogeochemical cycles, with a specific focus on understanding how climate change, disturbance, and invasion impact ecosystem structure, function, and services.

FELLOWSHIPS

Graduate Division Completion Fellowship, UCI
Fall 2021, $12,000

Ridge to Reef Graduate Fellowship, UCI
2020-2021, $34,000

Ridge to Reef Graduate Fellowship, UCI
2018-2019, $34,000

PUBLICATIONS

Fiore, N.M., Goulden, M., Czimczik, C.I., Pedron, S.A., and Tayo, M. (2020) Do recent NDVI trends indicate boreal forest decline? *Environmental Research Letters, Volume 15, Number 9.*

PRESENTATIONS

Fiore, N.M. (2021) "Soil properties in response to vegetation type." Oral presentation at Irvine Ranch Conservancy Speaker Series: Loma Ridge Global Change Experiment.

Fiore, N.M., Goulden, M. (2020) "The effects of experimental drought and nitrogen addition on above and belowground carbon pools in Mediterranean grasslands and coastal sage scrub." Poster presentation at UCI Environmental Research Symposium 2020.

Fiore, N.M., Goulden, M., Czimczik, C.I., Pedron, S.A., and Tayo, M. (2019) "Do recent NDVI trends indicate boreal forest decline?" Poster presentation at NASA Arctic-Boreal Vulnerability Experiment Team Meeting 2019.

Fiore, N.M., Goulden, M., Czimczik, C.I., Pedron, S.A., and Tayo, M. (2018) "Composition and structure of browning and greening forests in interior Alaska." Poster presentation at AGU Fall Meeting.

Fiore, N.M., Goulden, M. (2018) "Building connections with land managers to promote ecosystem services in Southern California." Poster presentation at NSF Research Traineeship Annual Meeting.

Fiore, N.M., Czimczik, C.I., Pedron, S.A., Elder, C.D., and Goulden, M. (2018) "Forest composition, structure and productivity of browning and greening forests in Interior Alaska." Poster presentation at NASA Arctic-Boreal Vulnerability Experiment Team Meeting 2018.

Fiore, N.M., Goulden, M. (2017) "Towards optimizing land management for carbon sequestration and other ecosystem services in the face of climate change." Poster presentation at UCI Environmental Research Symposium 2017.

RESEARCH EXPERIENCE

Goulden Lab, UCI Department of Earth System Science Irvine, CA.
Graduate Student Researcher, 2016-2022

- Evaluated the response of soil properties, and above and belowground biomass pools to drought and nitrogen deposition in a large-scale, long-term experiment in Mediterranean shrub and invasive grassland ecosystems.
- Examined the effects of fire and succession on satellite-derived NDVI in Alaskan boreal forests by combining field data with remote sensing.
- Mentored and managed over 15 undergraduate interns and volunteers, and 2 citizen science volunteers.

National Audubon Society Starr Ranch Trabuco Canyon, CA.
Restoration and Invasive Species Control Technician, 2013-2015

- Conducted research-based invasive species control and native restoration in the riparian corridor of a 4,000 acre reserve.

- Designed and implemented climate-smart restoration projects using locally collected seeds and cuttings.
- Mapped and tracked invasive spread using GIS.
- Completed endangered species habitat assessments and created proposals for critical habitat designation.
- Led over 30 all-ages volunteer events, and 10 environmental education days for kids.

UCSC Sinervo Behavioral Ecology Lab Santa Cruz, CA.
Animal Husbandry Intern, 2013

- Investigated behavioral ecology and response to climate change in western side blotched lizards.
- Processed and handled ~200 gravid female lizards, collected eggs, hatched juveniles, and collected data on hatchlings.

UCSC Small Mammal Research Lab Santa Cruz, CA.
Small Mammal Research Intern, 2012-2013

- Investigated habitat stratification and population dynamics of small mammals.
- Assisted in ~10 field trappings, collected data, entered data, and analyzed statistics.

COMMITTEES, COUNCILS, AND VOLUNTEER WORK

Diverse Educational Community and Doctoral Experience, UCI Volunteer, 2017-2019
Ridge to Reef Leadership Council, UCI Council Leader, 2018-2019
UCSC Carbon Fund Grant Council Council Member, 2012-2013
UCSC Campus Sustainability Council Council Member, 2011-2012

ABSTRACT OF THE DISSERTATION

Ecosystem Resilience to Global Environmental Change

by

Nicole Marie Fiore

Doctor of Philosophy in Earth System Science

University of California, Irvine, 2022

Professor Michael Goulden, Chair

Global environmental change is impacting ecosystems. Drought, nitrogen deposition, and invasion by annual grasses (GL) are causing extensive loss of Southern California's coastal sage scrub (CSS) community. Warmer temperatures, changes in precipitation, and altered fire regimes are impacting interior Alaska’s boreal forest function and productivity. In this dissertation, I explore these two contrasting ecosystems with the goal of developing a mechanistic understanding of how ecosystems respond to multiple global environmental change drivers.

Chapter 2 examines an apparently stable vegetation boundary between CSS and GL. This chapter utilizes historical aerial photography and measures of above and belowground properties to examine how vegetation type impacts soil development. CSS had more deeply distributed root biomass, denser surface soil, and greater total stocks of soil organic carbon and nitrogen than GL. Vegetation type creates unique soil properties that may reinforce the stable boundary by preventing invasion of vegetation with different growth, rooting, and/or water-use strategies.

Chapter 3 explores how CSS and GL respond to drought and added nitrogen. CSS was more sensitive to global change than GL and drought was the main driver of ecosystem change.

In CSS, drought and drought × +N reduced native shrub biomass and altered litter composition, consistent with a vegetation shift from CSS to GL. These changes were mirrored belowground, with reductions in soil bulk density, soil organic carbon content, and soil C/N ratio in CSS drought plots. The surface soil properties in CSS drought plots were more similar to GL than to CSS, indicating that drought induced vegetation shifts from CSS to GL impact ecosystem properties and processes, both above and belowground.

Chapter 4 combines measures of remotely-sensed NDVI with forest surveys to explore the drivers of recent NDVI trends. Recent fire led to sharp NDVI decreases, while early recovery of deciduous species led to NDVI increases. The mid-succession transition from deciduous to evergreen forests led to weak NDVI decreases, and the mid-to-late successional thinning of evergreen canopies to weak NDVI increases. Thus, both increasing and decreasing NDVI stands occur naturally across the landscape, and do not necessarily reflect a large-scale shift in boreal forest productivity.

Chapter 1.

Introduction

1.1 Global environmental change in sensitive ecosystems

The magnitude and extent of projected global changes in the 21st century are likely to have profound impacts on the functioning of Earth's ecosystems. Ecosystem response to global change is a key component of ecosystem resilience, or the ability of an ecosystem to return to stability after perturbation. Ecological theory states that ecosystems with lower resilience are more sensitive to change and display a greater likelihood of transitioning to an alternative stable state when faced with high magnitude or extended disturbance (Laycock, 1989; Laycock, 1991; Seddon et al., 2016). Accurate prediction of the structure and functioning of future ecosystems requires mechanistic understanding of ecological responses to change. Two ecosystems are explored in this dissertation. First, the Mediterranean coastal sage scrub (CSS) and grassland (GL) communities in Southern California are investigated in Chapter 2 and Chapter 3. Next, the boreal forests of interior Alaska are examined in Chapter 4. Although these contrasting ecosystems have little in common, they both have been highlighted in recent research due to their high sensitivity to global change (Seddon et al., 2016).

Southern California represents an area where drought, nitrogen deposition, and fire disturbance may interact with ecosystem resilience. Of particular interest is the coastal sage scrub community (CSS), known for its high species diversity and endemism, as well as it's drought resistance and adaptations to frequent fire (Cleland et al., 2016). Despite these adaptations to global change, widespread loss of CSS habitat has been documented across California, with studies

estimating only 10% of its original extent still intact (Rundel, 2007; Talluto and Suding, 2008). Several studies have indicated that invasion by non-native, annual GL species is the largest threat to the CSS ecosystem (Freudenberger et al., 1987; Minnich and Dezzani, 1998). We employed a large-scale, long-term, multifactorial precipitation and nitrogen manipulation experiment in adjacent CSS and GL communities to investigate how these vegetation communities impact soil development and explore their responses to long-term global change, both above- and belowground.

The boreal forests of Alaska represent an area where warmer temperatures, changes in precipitation, and altered fire regimes may interact with forest productivity and ecosystem succession. The remote and rugged nature of the boreal forests traditionally made long-term, large-scale field research difficult, but advances in technology and data science have allowed us to employ new methods using satellite-derived imagery to study this important landscape from afar. We utilized satellite-derived Normalized Difference Vegetation Index (NDVI; a proxy for forest productivity) combined with forest surveys of Alaskan boreal forests throughout succession to explore the impacts of forest properties on NDVI, and to determine the drivers of changes in NDVI.

This dissertation aims to answer the following research questions:

In Southern California:

1. What are the potential drivers of stable CSS/GL boundaries?
2. How does vegetation type (shrub vs. grass) impact soil properties along the stable boundary?

3. How do drought and nitrogen addition impact CSS and GL communities above and belowground?

4. Can global change alter the stability of the CSS/ GL boundary?

In the boreal forests of Alaska:

1. How are changes in forest structure and composition in recently burned stands associated with NDVI decreases?
2. How are changes in forest structure and composition in young stands associated with NDVI increases?
3. In the absence of recent fire, how are NDVI decreases in mid-to-late successional forests related to forest structure and composition?
4. In the absence of recent fire, how are NDVI increases in mid-to-late successional forests related to forest structure and composition?

1.2 Vegetation mosaics in Southern California

Over the course of the last two centuries, native Californian shrublands, grasslands, and forblands have been invaded by non-native annual grasses from Eurasia. (Talluto and Suding, 2008). Early settlers originally brought these annual grass species (mostly from the *Bromus* and *Avena* genuses) for food, medicinal, and ornamental purposes (Hendry, 1931; Hobbs, 1983; Mooney et al., 1986). Annual grasses became aggressive competitors in their new environment, and studies estimate that annual grasses now cover 2.9 million hectares of California. These invasions not only trigger the loss of native species diversity, but also cause permanent disruptions to ecosystem structure and function, especially when the invasion changes the dominant life form

(i.e., shrub to grass) (D'Antonio and Vitousek, 1992; Vitousek et al., 1997; Mooney and Hobbs, 2000; Talluto and Suding, 2008).

The CSS/GL mosaic is common to Southern California, and often exists across relatively uniform physical conditions, with many mosaics displaying remarkable stability. The stability of the vegetation boundaries between CSS/GL suggests that underlying mechanisms, whether abiotic or biotic, provide some form of ecological resistance, preventing expansion of either shrub or grass across the boundary. In the second chapter of this dissertation, I investigate a stable vegetation boundary between CSS and GL at the Loma Ridge Global Change Experiment (LRGCE) to explore the possible drivers of the boundary stability.

The existence of adjacent vegetation communities of differing life forms (shrub vs. grass) also provides an opportunity to explore how different vegetation types impact the development of the soil along the boundary. Early research in pedogenesis by Hans Jenny proposed that soil formation was the function of five state factors: climate, organisms, parent material, and time (Jenny, 1941;1958). As the state factors between the CSS and GL communities are similar, we can employ a biosequence study to focus on the impact of organisms, specifically vegetation (grass or shrub) on soil formation. If the soil properties below GL and CSS are significantly different, could these soil properties interact with the vegetation to influence the boundary stability?

1.3 Global change impacts in Southern California

Urbanization, drought, nitrogen deposition, and altered fire regimes are frequently cited as the main global change drivers responsible for habitat loss in California (Talluto and Suding, 2008). Studies have shown that these global change drivers often interact with CSS ecosystem invasibility to trigger large-scale vegetation type shifts from native CSS to non-native, annual GL.

Talluto and Suding (2008) estimated that 49% of the area previously covered by CSS had been converted to invasive Eurasian grassland between 1930 and 2005, and only 15% remained uninvaded.

In Chapter 3, I explore both the long-term, and combined effects of drought and nitrogen addition on above and belowground properties in adjacent CSS and GL at the LRGCE. Mechanistic understanding of how vegetation and soils respond to drought, nitrogen addition, and the associated vegetation shifts between CSS and GL is required to accurately predict how these ecosystems will function in the future.

1.4 Vegetation dynamics in the boreal forest

The boreal forest covers roughly 17% of the Earth's land surface and contains more than 30% of all carbon stored in the terrestrial biome (Kasischke and Stocks, 2012). Climate is changing rapidly in the high-latitude regions of the northern hemisphere, and warmer temperatures, changes in precipitation, and larger and more frequent fires have been documented across the boreal regions (Beck and Goetz, 2011; Kasischke and Stocks, 2012). Boreal forest health and productivity are intimately linked to climate variables. Studies indicate that warmer temperatures and longer growing seasons are enhancing boreal forest productivity, while moisture stress and too high temperatures are reducing productivity and increasing tree mortality (Goetz et al., 2005).

Remote sensing is a valuable tool for studying the composition and productivity of this vast and often inaccessible region, and many studies have utilized satellite-derived measurements of normalized difference vegetation index (NDVI) to infer landscape-scale productivity. Time series are used to calculate NDVI trends over time, and previous studies documented widespread NDVI decreases across boreal forest regions and NDVI increases in tundra regions, which was

linked to climate change related changes to productivity (Goetz et al., 2005; Beck and Goetz, 2011). In Chapter 4, we combine forest surveys with measures of satellite-derived NDVI to explore NDVI trends across the Alaskan landscape, and to determine how forest properties impact NDVI. Our results highlight the importance of deconvolving the legacy effect of disturbance and recovery when diagnosing trends in ecosystem structure and function.

1.5 References

Beck, P. S. A. and Goetz, S. J. (2011) Satellite observations of high northern latitude vegetation productivity changes between 1982 and 2008: ecological variability and regional differences *Environ. Res. Lett.* 6 045501

Cleland, E. E., Funk, J. L., & Allen, E. B. (2016). Coastal Sage Scrub. In *Ecosystems of California* (pp. 429-448). University of California Press.

D'Antonio, C. M., & Vitousek, P. M. (1992). Biological invasions by exotic grasses, the grass/fire cycle, and global change. *Annual review of ecology and systematics*, *23*(1), 63-87.

Goetz, S. J., Bunn, A. G., Fiske, G. J. and Houghton R. A. (2005) Satellite-observed photosynthetic trends across boreal North America associated with climate and fire disturbance *Proc. Natl Acad. Sci.* 102 13521–5

Hendry, G. W. (1931). The Adobe brick as a historical source: reporting further studies in adobe brick analysis. *Agricultural History*, *5*(3), 110-127.

Hobbs, E. R. (1983). *Factors controlling the form and location of the boundary between coastal sage scrub and grassland in southern California* (Doctoral dissertation, University of California, Los Angeles).

Jenny, H. (1941). Factors of soil formation. McGraw-Hill, New York. *Factors of soil formation. McGraw-Hill, New York.*

Jenny, H. (1958). Role of the plant factor in the pedogenic functions. *Ecology*, *39*(1), 5-16.

Kasischke, E. S., Christensen, N. L. and Stocks, B. J. 1995 Fire, global warming, and the carbon balance of boreal forests *Ecol. Appl.* **5** 437–51

Mooney, H. A., Hamburg, S. P., & Drake, J. A. (1986). The invasions of plants and animals into California. In *Ecology of biological invasions of North America and Hawaii* (pp. 250-272). Springer, New York, NY.

Mooney, H. A., & Hobbs, R. J. (2000). Global change and invasive species: where do we go from here? *Invasive species in a changing world. Island Press, Washington, DC*, 425-434.

Seddon, A. W., Macias-Fauria, M., Long, P. R., Benz, D., & Willis, K. J. (2016). Sensitivity of global terrestrial ecosystems to climate variability. *Nature*, *531*(7593), 229-232.

Talluto, M.V., Suding, K.N. (2008). Historical change in coastal sage scrub in southern California, USA in relation to fire frequency and air pollution. *Landscape Ecol* 23, 803–815.

Vitousek, P. M., D'antonio, C. M., Loope, L. L., Rejmanek, M., & Westbrooks, R. (1997). Introduced species: a significant component of human-caused global change. *New Zealand Journal of Ecology*, 1-16.

Chapter 2.

Drivers and implications of a stable shrubland grassland boundary in Southern California

2.1 Abstract

In this study, we investigate the spatiotemporal dynamics of an abrupt boundary between two common vegetation types in coastal California, coastal sage scrub (CSS) and annual grassland (GL) and explore how vegetation types and soils interact to control associated belowground properties. We combine historical aerial photography of the boundary with measures of vegetation community structure and soil properties to determine how root biomass, soil texture, bulk density, organic carbon and nitrogen content and distribution, and C/N ratio relate to vegetation type. Our historical imagery investigation indicates that the boundary has been stable for over 80 years despite disturbances such as frequent wildfire and historic drought. We found that overlying vegetation type impacted most belowground properties near the surface (0-10 cm) and below depths of 50 cm. Overall, CSS soils had 145% more total root biomass, 30% more total soil organic carbon stocks, 10% more soil nitrogen stocks, and significantly denser surface soils than GL. The distribution of these properties varied with vegetation type, with CSS showing deeper and more heterogeneous distributions than GL. Our results confirm that different vegetation types (shrub or grass) create unique plant-soil systems that can impact soil properties which we believe may further reinforce the stability of the vegetation boundary.

2.2 Introduction

The native coastal sage scrub (CSS) and non-native annual grassland (GL) vegetation mosaic is commonly found throughout the Mediterranean climate region of California. Early California settlers originally brought non-native grasses for food, medicine, and ornamental purposes, which spread quickly throughout the state (Mooney et al., 1986). Extensive agriculture, ranching, and urbanization further altered native landscapes and led to the widespread conversion of native shrublands, grasslands, and forblands to annual non-native grassland as early as the late 18th century (Hendry, 1931; Hobbs, 1983; Talluto and Suding, 2008). These conversions not only triggered the loss of native species, but also caused permanent disruptions to ecosystem structure and function, particularly when the conversion changed the dominant life form (i.e., shrub to grass) (D'Antonio and Vitousek, 1992; Vitousek et al., 1997; Mooney and Hobbs, 2000; Talluto and Suding, 2008).

The boundary dynamics between shrub- and grasslands in arid and semi-arid climates have been the focus of scientific debate for decades (Laycock, 1989; Westoby et al., 1989; Laycock, 1991; Mueller et al., 2007). Livestock grazing was thought to be the main control on shrub- and grassland boundaries, and release from grazing disturbance would push the ecosystem towards the stronger competitor, leading to a singular climax community of either shrub- or grassland (Westoby et al., 1989). The boundaries between shrub- and grasslands are often dynamic. In the American Southwest, expansion of woody shrubs into grasslands is well documented, while other shrublands in Southern California are experiencing invasion by annual grasses (Talluto and Suding, 2008). Yet several boundaries between native shrub and non-native grassland communities in California have been documented to display remarkable stability despite cessation of grazing (Hobbs, 1983; Davis and Mooney, 1985). In this study, we investigate a boundary

between CSS and GL to explore the spatiotemporal boundary dynamics and to determine the impact of the contrasting vegetation types on belowground properties.

The CSS habitat is dominated by native, slow growing, perennial woody shrubs such as California coastal sage (*Artemisia californica* Less.), laurel sumac (*Malosma laurina* Nutt.), and black sage (*Salvia mellifera* Greene) (Cleland et al., 2016). This habitat is known for its high species diversity and endemism (Noss et al., 1995), as well as its adaptations to frequent drought and wildfire (Cleland et al., 2016). Shrub systems are known for their high heterogeneity in plant biomass aboveground, which is mirrored belowground. In shrub systems, soil development is concentrated directly under the shrub canopies, leading to higher concentrations of soil resources under canopies compared to bare areas outside of the canopy (Schlesinger et al., 1996; Schelsinger and Pimanis, 1998; Bird et al., 2000). Shrub systems have a shallow network of small roots, and large, deep tap roots (as deep as 4 m in CSS) that evolved to access deep water tables and avoid root overlap with other plants, which often leads to deeper soil development and more deeply distributed nutrients (Veneklas and Poot, 2003; Jobbágy and Jackson, 2000).

In contrast, the annual GL habitat in Southern California has high density, non-native annual grasses such as *Bromus diandrus* Roth, *Avena fatua* Peterm., and *Lolium multiflorum* Lam. (Biswell, 1956). These species are known to invade areas of bare soil in suitable climates across California and can quickly dominate landscapes that have been recently disturbed (Germino et al., 2016). GL habitats often display high homogeneity, with herbaceous grasses covering nearly 100% of the surface. (Germino et al., 2016; Kimball et al., 2014). These aboveground trends are mirrored belowground, and GL is known to have more homogenous distributions of roots, soil properties, and nutrients (Schlesigner et al., 1996; Germino et al., 2016). GL also tends to be more shallowly

rooted (within the top 50 cm) than shrub or tree systems, meaning that most plant inputs to the soil are concentrated in the topsoil (Jobbágy and Jackson, 2000).

The goal of our study was to explore the spatiotemporal dynamics of the boundary as well as the vegetation and soil properties in the CSS and GL communities to determine the impact of vegetation type on soil development. These contrasting life forms (shrub vs. grass) with differing life history strategies (perennial vs. annual) and growth forms (deep-rooted, woody shrub vs. shallow-rooted, herbaceous) likely impact soil development in unique ways. We utilized historical aerial photography of the site combined with measures of above- and belowground vegetation as well as measures of soil bulk density, organic carbon (SOC) and nitrogen (N) content and distribution, and C/N ratio to two meters depth to examine the soil properties across the vegetation boundary. We hypothesize that the boundary is maintained by ecological factors, namely vegetation types. We predict that the differences in soil properties between the vegetation types will largely be related to differences in rooting strategy, with soils in CSS showing deeper and more heterogeneous development, while soil in GL will show shallower, more homogenous development.

2.3 Methods

Study site

All data was collected in ambient plots located at the Loma Ridge Global Change Experiment (LRGCE) on a gentle (~10%), northwest facing slope at the foothills of the Santa Ana Mountains (117.704 W, 33.742 N) of Southern California, U.S.A. The LRGCE, started in 2006, examines the effects of global change on adjacent Mediterranean CSS and annual GL plots, found along an apparently stable boundary (See Potts et al., 2012 for complete description of

experiment). The study site experiences a Mediterranean climate, characterized by warm, dry summers and mild, wet winters. The annual average high temperature is 24.1 ℃ and the annual average low is 9.7 ℃. The yearly mean average precipitation is 327 mm, and generally falls in the months of November-April. The soil at the study site is classified as loamy, mixed, thermic *Typic Palexeralfs* (California Soil Resource Lab, http://casoilresource.lawr.ucdavis.edu) (Khalili et al., 2016) (Table 1). The soil formed on a several-meter-deep colluvial deposit eroded from sedimentary rock of the Vaqueros formation, with no obvious topographical distinctions between vegetation types (Potts et al., 2012, Khalili et al., 2016).

Boundary investigation

Aerial photographs spanning the available historical record of the site were downloaded from the UC Santa Barbara Library (http://mil.library.ucsb.edu/apcatalog). Photos with a clear view of the study site were available from 1939, 1977, 2002, and 2020. The photos were then georeferenced in ArcGIS Pro using a first order polynomial from control points set on stable geographic features common to all photos. Each photo contained at least 10 control points. We then plotted the vegetation boundary line on the World Imagery base map and compared boundary location with each georeferenced historical photo. We used a digital elevation model in ArcGIS Pro to calculate elevation, slope, and aspect within the CSS and GL plant communities.

Vegetation cover and composition

We measured fractional species composition and cover during peak growing season in March of 2020. In CSS, species composition and cover were measured as fractional cover by species over total area in each plot. In GL, species composition and cover were measured using point intercepts, where two 160 × 60 cm^2 polyvinyl chloride frames with 10-cm interval grids were

positioned within each plot. The first-intercepted species found at each grid point was recorded, and if no species were found, the point was recorded as plant litter or bare soil. The number of interceptions for each plant species was then summed within each plot to calculate fractional cover.

Vegetation live biomass and litter pools

Live herbaceous biomass and litter were collected from each plot in March 2020. Four 14 cm by 50 cm polyvinyl chloride frames were placed in each plot, and all live herbaceous biomass encountered within the frame was clipped to the soil surface, sorted by type (grass or forb) and collected. Litter was then collected within each frame and sorted by type (grass, forb, or shrub leaf and woody debris). All biomass and litter samples were taken back to the lab, dried at 65℃ for four days, and weighed.

The volume of all individual shrubs within a four by four meter center subplot was calculated in CSS plots in March 2020 using measurements of height, and two perpendicular width measurements, assuming a spherical shape. Shrub volume was then converted to biomass using species specific volume-mass relationships (Pasquini, 2008; Table A.6)

Soil texture

In 2011, we took samples from one soil core to two meters depth at a pre-selected point within each plot using a 5.7 cm diameter soil auger (N=8 for each vegetation type) to measure soil texture. If the point fell directly on a shrub stem, the point was shifted to the nearest location away from the stem. Each soil core was separated into the following depth ranges: 0-15 cm, 15-30 cm, 30-45 cm, 45-100 cm, and 100-200 cm. Samples were dried at 105℃ and sieved. We then added 150 mL of a 17 g/L sodium hexametaphosphate solution to the soil, and samples were agitated on a horizontal shaker for 60 minutes. Samples were brought to a constant volume of 1 L with

deionized water in a graduated cylinder, mixed, and the density of the suspension was measured with a hydrometer after 40 seconds to determine the silt plus clay fraction and after two hours to determine the clay fraction.

Soil core sampling

In spring of 2020, we took samples from one soil core to two meters depth at a pre-selected point within each plot using a 5.7 cm diameter soil auger (N=8 for each vegetation type) for biogeochemical analysis. If the point fell directly on a shrub stem, the point was shifted to the nearest location away from the stem. Each soil core was separated into the following depth ranges: 0-10 cm, 10-20 cm, 20-30 cm, 30-50 cm, 50-100 cm, 100-150 cm, and 150-200 cm. All soil cores were taken back to the lab and dried at 105°C to constant mass. Bulk density was calculated as the total mass of dry soil per volume of depth range. Soils were sieved to 2 mm and root biomass was collected from each soil core per depth range, and then was washed, dried and weighed. A small subsample of sieved soil was then pulverized. An aliquot was then analyzed for its SOC and N content (NC Soil Analyzer 2400, Thermofisher).

Statistical analyses

All aboveground properties were compared between vegetation types using student's t tests. Belowground properties were analyzed using a two-way analysis of variance to explore the effects of vegetation type, depth, and their interactions. If the main effects or their interaction were significant, we used student's t tests to explore the effect of vegetation type on the properties at each depth range. Data were square root transformed where necessary to improve normality and reduce heteroscedasticity.

2.4 Results

Boundary investigation

The vegetation boundary between CSS and GL at our study site is abrupt, with little transition zone. The two vegetation types occur on similar topography, parent material, and soil type (Table A.1), and show no indications of different climate or burn history. The aerial photos demonstrate that the boundary between CSS and GL has been stable since at least 1939, as evidenced by the earliest known historical photo of the site (Figure 2.1). The boundary between CSS and GL has remained remarkably stable despite wildfires in 2020, 2007, 1998, 1967, 1948, and 1914 (CAL FIRE, Fire and Resource 16 Assessment program, http://frap.cdf.ca.gov/), as well as historic drought conditions in 2012-2016, 1987-1992, and 1976-1977 (Western Regional Climate Center, https://wrcc.dri.edu/).

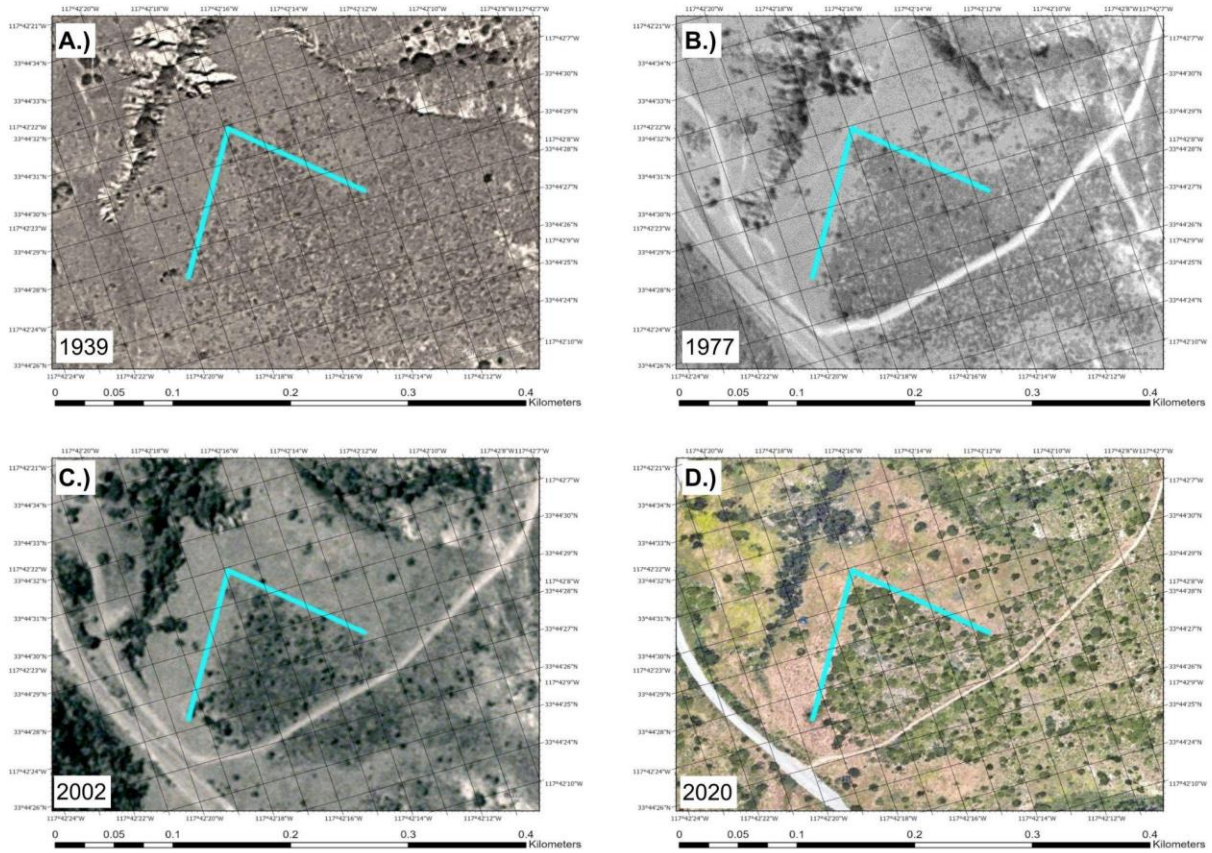

Figure 2.1. Aerial photos of the study site demonstrating the stable boundary between grassland and shrubland vegetation types. The blue line displays the vegetation boundary, with coastal sage scrub below the line, and grassland above the line. A.) Aerial photo of the experimental site in 1939 (University of California, Santa Barbara Library, Aerial Flight C-5925, http://mil.library.ucsb.edu/apcatalog). B.) Aerial photo of the experimental site in 1977 (University of California, Santa Barbara Library, Aerial Flight TG-7700 C.) Satellite image of experimental site in 2002 (Google Earth, 2002, http://earth.google.com/web/). D.) Satellite image of the Loma Ridge experimental site in 2020 (Google Earth, 2020, http://earth.google.com/web/).

Composition and cover of vegetation types

The CSS vegetation cover was characterized by higher species diversity, and a greater number of plant functional types, but also featured larger fractional cover of bare ground than GL (Figure 2.2). The vegetative cover in CSS averaged 60.5 ± 26.9% native shrub, 20.9 ± 18.7% invasive grasses, 0.7 ± 1.4% native grass, 4.7 ± 5.8% forb, and 13.1 ± 8.2% contained no vegetation

cover. The ground cover was 56.4 ± 41.1% leaf litter, 14.9 ± 17.1% woody debris, 13.5 ± 29.5% grass litter, and 15.1 ± 20.8% bare ground (Figure 2.2). GL vegetation cover was characterized by high density coverage of invasive Eurasian grasses that averaged 93.9 ± 5.6%, 2.5 ± 3.6% forb, 2.3 ± 6.1% native grass, and only 1.3 ± 2.6% contained no vegetation cover. The ground cover was mostly grass litter (88.3 ± 19.0%), 9.8 ± 16.5% forb litter, and 1.8 ±2.7% bare ground.

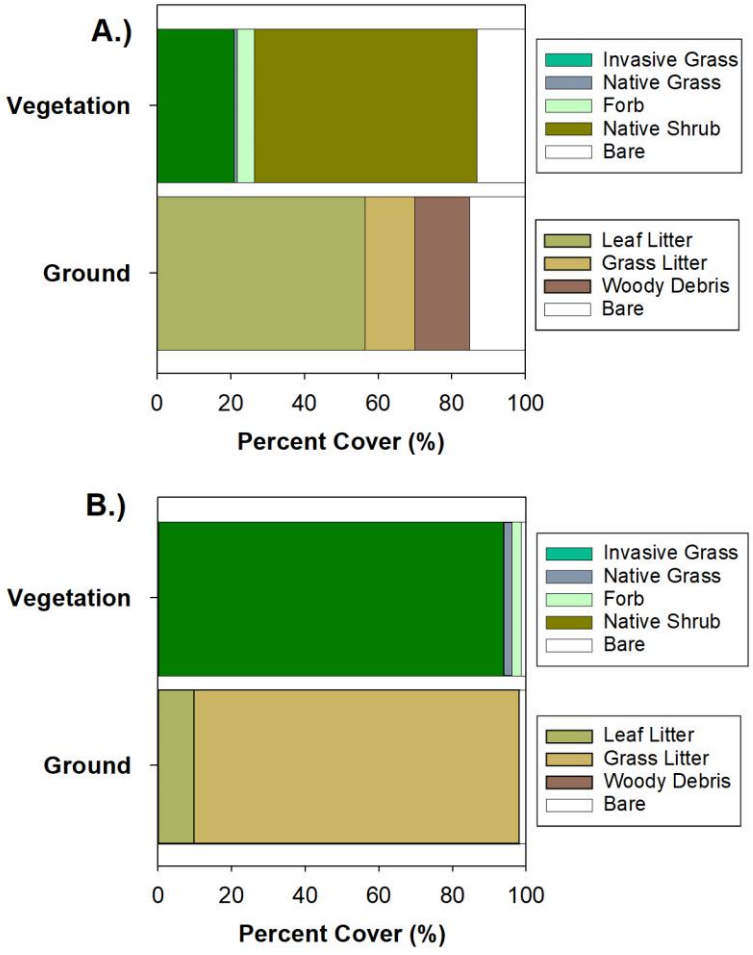

Figure 2.2. Average species composition and percent of vegetation cover and ground cover for the 2019-2020 growing year for Coastal Sage Scrub (CSS) and Grassland (GL) vegetation types at Loma Ridge, California. A.) CSS average species composition and cover. B.) GL average species composition and cover.

Live and Litter mass

Total live aboveground biomass was five times greater in CSS than GL, largely due to the presence of woody shrubs. Small amounts of grass and forb biomass were found in CSS (Figure 2.3A). Aboveground biomass in GL was purely herbaceous and was dominated by invasive grasses (Figure 2.3B). Litter pools were roughly four times greater in CSS than GL. CSS litter pools were dominated by shrub leaf litter and coarse woody debris, and small amounts of herbaceous litter, while GL litter was purely herbaceous (Figure 2.3A and 2.3B; Table A.3).

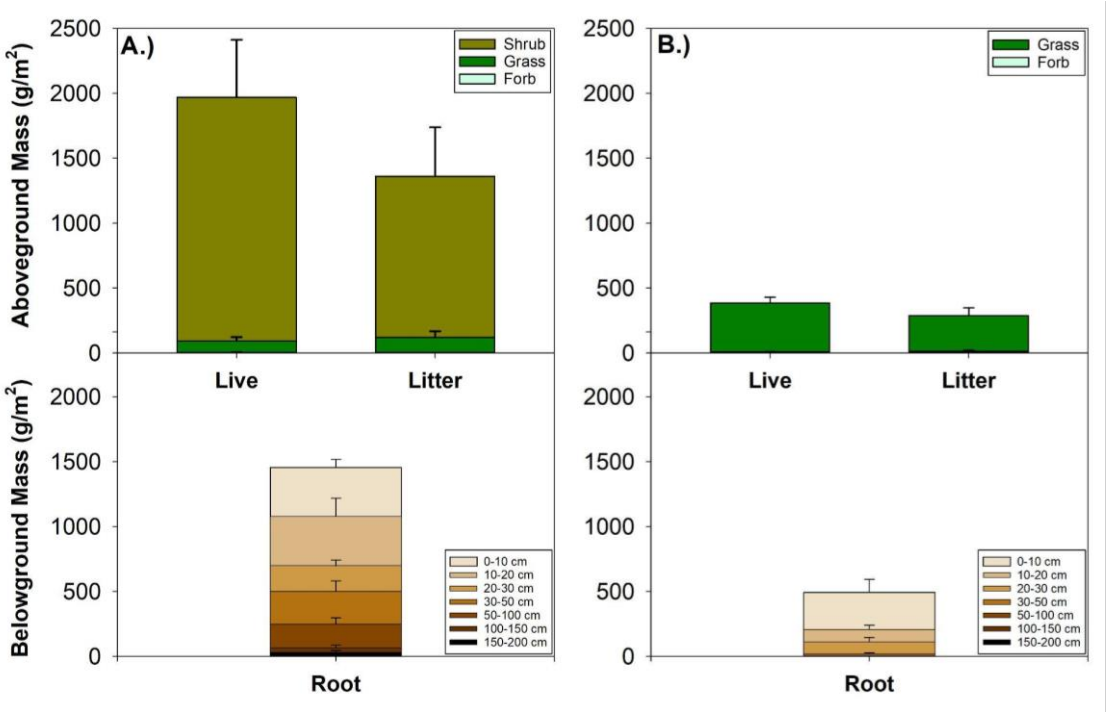

Figure 2.3. Average above and belowground live biomass and litter pools by type for the 2019-2020 growing year for Coastal Sage Scrub (CSS) and Grassland (GL) vegetation types at Loma Ridge, California. Error bars indicate standard error of the mean. A.) CSS average aboveground live biomass and litter by type, and average belowground root biomass. B.) GL average aboveground live biomass and litter by type, and average belowground root biomass.

Root biomass and distribution

Root biomass was highly variable in both vegetation types, CSS had three times greater total root biomass than GL (p=0.0141) (Figure 2.4A and 2.4B). In CSS, roots displayed a deeper distribution with 28% of total roots found in 0-10 cm, 23% in 10-20 cm, 14% in 20-30 cm, 17% in 30-50 cm and over 15% of roots were found below 50 cm in CSS (Figure 2.5B). CSS roots contained a mix of fine, herbaceous roots (<1 mm diameter) and thicker, woody roots (1-3mm diameter) from 0-30 cm, and only woody roots below 30 cm depth (Figure 2.8). In contrast, GL displayed a shallower distribution of root biomass, with 52% of total root biomass found in the top 10 cm of soil, followed by 18% in 10-20 cm, 22% in 20-30 cm, and only 7% between 30-50 cm (Figure 2.4B). No roots were found in GL beyond 50 cm. Roots in GL consisted of dense webs of fine (<<1 mm diameter), herbaceous roots, that indicated high amounts of both vertical and horizontal spread that was largely limited to the top 10 cm of depth (Figure 2.8, Figure 2.4B).

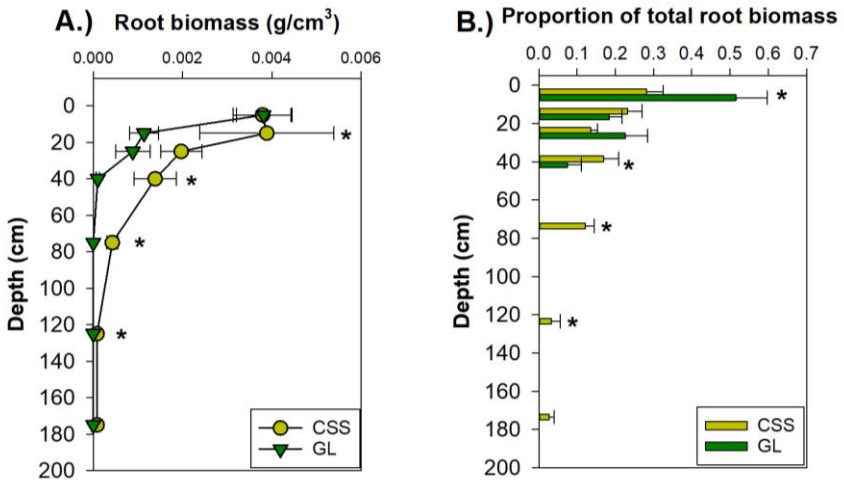

Figure 2.4. A.) Root biomass and B.) Distribution of root biomass as measured by proportion of total biomass found in each depth layer (interval root biomass/ total root biomass) Error bars indicate standard error of mean. Asterisks indicate statistical difference between vegetation types at that depth at P<0.05.

Soil properties

The soil texture was consistent with depth and between CSS and GL vegetation types (Figure 2.5). The soil was composed of mostly sand in both vegetation types (Figure 2.5, Table A.2). The soil under CSS was significantly denser than GL between 0-30 cm (Figure 2.6A, Table A.4). We found that SOC in CSS displayed greater heterogeneity (CSS SD at 0-10 cm: 4.92 g C/kg soil) than GL, which displayed a more homogenous distribution (GL SD at 0-10 cm: 1.59 g C/kg soil). SOC content measured by mass (g C/kg soil) was significantly greater in CSS than GL at the surface (0-10 cm; p=0.033), and at depths greater than 50 cm (Figure 2.6B, Table A.4). When measuring SOC on a volumetric basis (g C/cm^3), the greater density of soil found in CSS had a multiplicative effect and further increased the differences in SOC content between the vegetation types (Figure 2.6C, Table A.4). Overall, CSS contained 29% more total SOC to 2 m than GL (p=0.012) (Figure 2.7A, Table A.5).

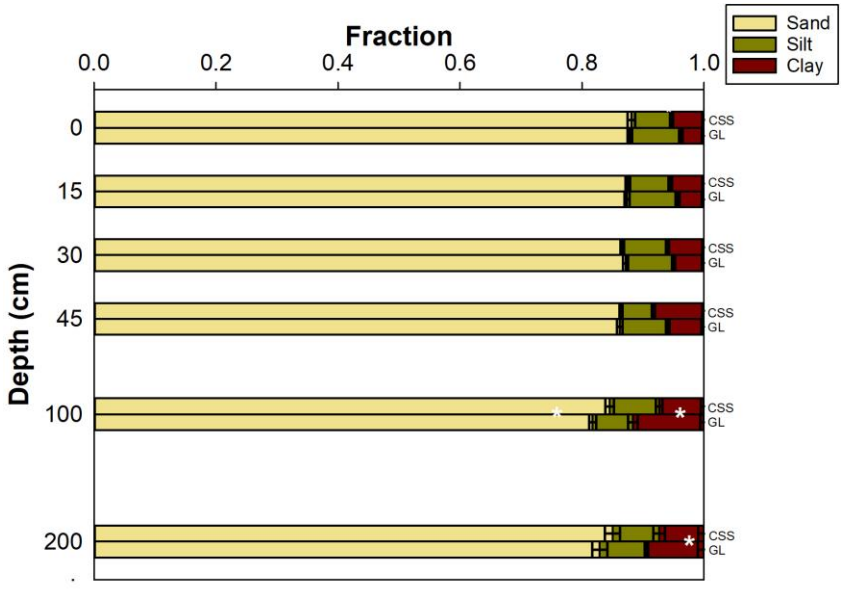

Figure 2.5. Soil texture as fractional composition of sand, silt, and clay to two meters depth in Coastal Sage Scrub (CSS) and Grassland (GL) vegetation types at Loma Ridge, California. Error bars indicate standard error of mean and white asterisks (*) indicate statistical difference between vegetation types at that depth at P<0.05.

Nitrogen content displayed similar trends as SOC, with high heterogeneity in CSS and homogeneity in GL (Figure 2.6F). Soil N measured by mass (g N/kg soil) was significantly higher in GL than CSS at the surface (0-10 cm; $p<0.001$) and at 30-50 cm ($p=0.046$), but CSS had higher N content at 150-200 cm ($p=0.007$) (Figure 2.6F). Volumetric N content (g N/cm^3) was similar near the surface in both vegetation types but was greater in CSS beyond 50 cm depth (Figure 2.6G). Soil N was more concentrated at the surface in GL, whereas CSS displayed a roughly equal distribution throughout depth (Figure 2.6H). Overall, CSS had 9% greater total soil N stocks to 2 m than GL ($p=0.018$) (Figure 2.7B). The C/N ratio was significantly greater in CSS than GL at 0-10 cm and 20-30 cm (Figure 2.6E, Table A.4).

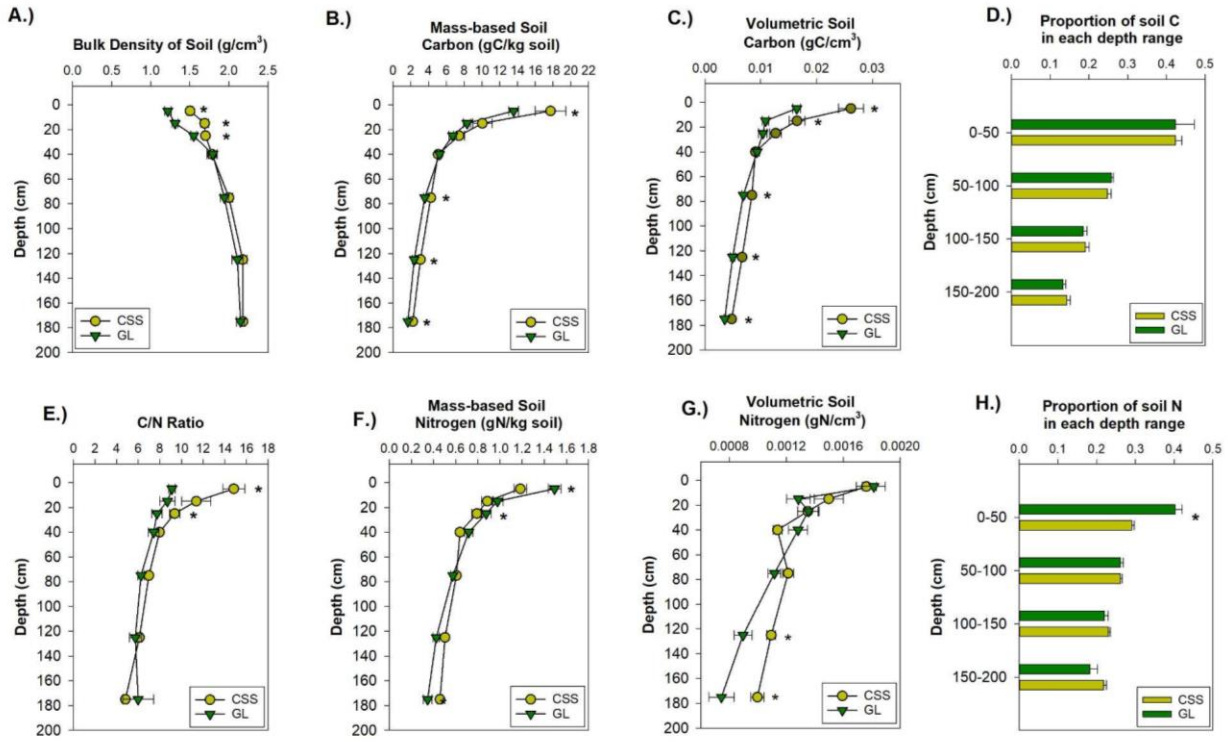

Figure 2.6. Soil properties for Coastal Sage Scrub (CSS) and Grassland (GL) vegetation types at Loma Ridge, California. Error bars indicate standard error of mean. Asterisks indicate statistical difference between vegetation types at that depth range at $P<0.05$. A.) Soil bulk density for each vegetation type. B.) Soil carbon content per weight soil for each vegetation type. C.) Volumetric soil carbon content for each vegetation type. D.) Vertical distribution of soil carbon as measured by proportion of soil carbon in each depth range (interval soil C/ total soil C) E.) Soil carbon to nitrogen ratio for each vegetation type. F.) Soil nitrogen content per weight soil for each vegetation type. G.) Volumetric soil nitrogen content for each vegetation type. H.) Vertical distribution of soil nitrogen as measured by proportion of soil nitrogen in each depth range (interval soil N/ total soil N).

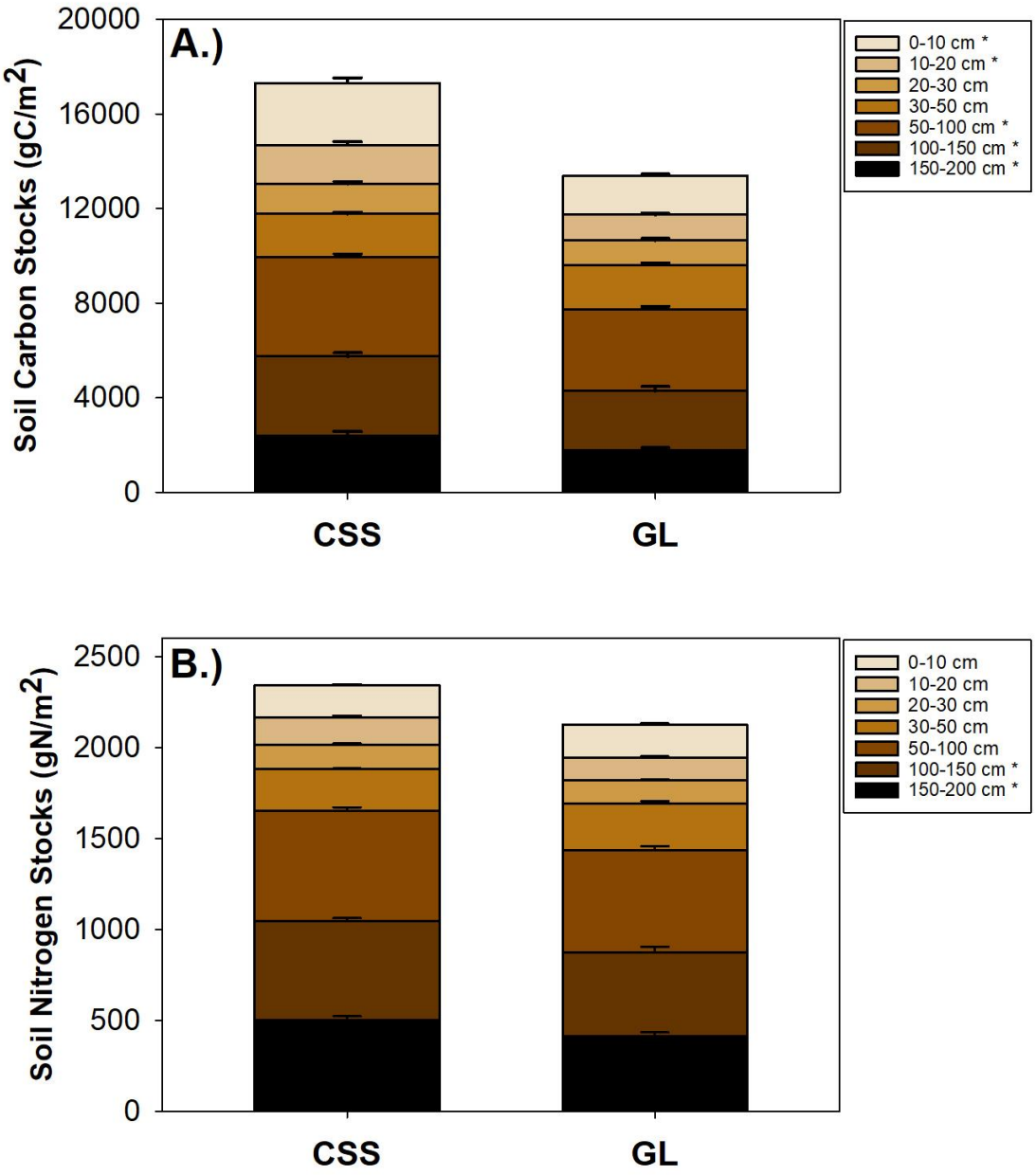

Figure 2.7. Total soil organic carbon and nitrogen stocks for Coastal Sage Scrub (CSS) and Grassland (GL) vegetation types at Loma Ridge, California. Error bars indicate standard error of mean and asterisks in legend indicate statistical difference ($p<0.05$) between vegetation types at that depth range. A.) Total soil organic carbon stocks by depth layer. B.) Total soil nitrogen stocks by depth layer.

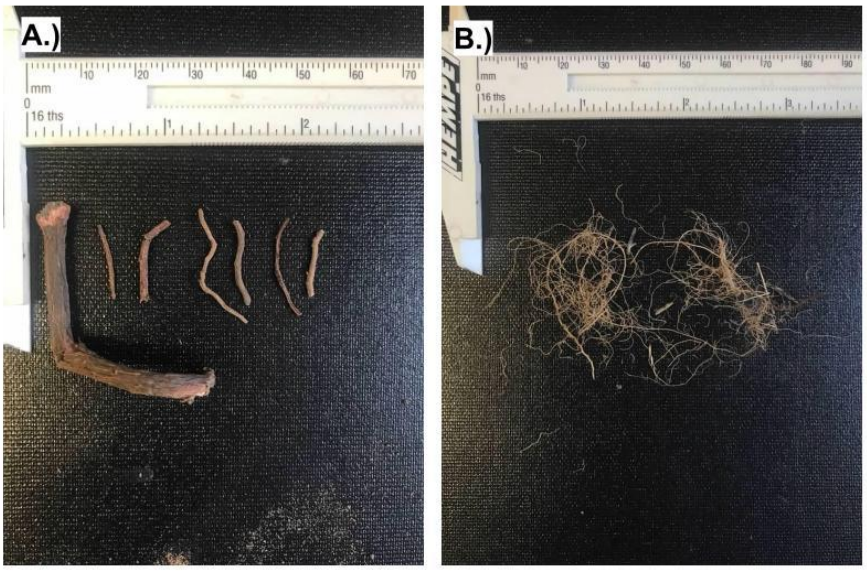

Figure 2.8. Root structures found in 0-10 cm depth range from A.) Coastal Sage Scrub (CSS) and B.) Grassland (GL) vegetation types at Loma Ridge, California where belowground properties were measured.

2.5 Discussion

Boundary stability

The vegetation boundary between GL and CSS at our site was stable throughout the available time period (1939-2020) (Figure 2.1). Our results for topography as well as soil type and texture show little difference between the vegetation types, which indicates that the boundary is likely maintained by ecological factors rather than abiotic conditions (Table A.1; Figure 2.2). Stable vegetation boundaries between GL and CSS are common throughout southern California, and several hypotheses exist to explain their stability, including differences in fire response (Schultz et al., 1955), animal herbivory (Davis and Mooney, 1985), water use strategies (Schultz et al., 1955; Davis and Mooney, 1985; Parker, 2019), and/or thermal gradients caused by shrub canopy shading (Davis and Mooney, 1985). Our results suggest that the differences in soil

properties associated with the overlying vegetation types may also reinforce boundary stability between CSS and GL.

Differences in rooting strategy between vegetation types

Our results for root biomass by depth display distinct differences in root architecture and distribution between CSS and GL, which we believe drive the depth dependent differences in soil properties. Overall, CSS had three times more total root biomass to two meters depth and roots were more deeply distributed than in GL (Figures 2.4A, 2.4B, and 2.5B). While there was no significant difference in root biomass between 0-10 cm depth, there were clear differences in root architecture near the surface (Figures 2.5 and 2.8). These differences in root biomass, distribution, and architecture are likely evidence of differing water-use strategies, where CSS has adapted to capture deeply stored water, while GL capitalizes on shallow water from recent rainfall (Schultz et al., 1955; Davis and Mooney, 1985; Parker, 2019).

Differences in soil properties between vegetation types

Soil bulk density differed greatly between the vegetation types, with soil in CSS being significantly denser than soil in GL between 0-30 cm depth. Soil bulk density is dependent on soil texture, soil mineral density and arrangement, root activity, and type and amount of organic matter (USDA NRCS, 2008). As soil texture and type were similar between vegetation types, the differences in bulk density are likely the result of differences in root type and architecture between CSS and GL near the surface. The fast growing, dense webs of fine roots of the annual grass species in GL may break up the soil each growing season (Hillel, 2004), leading to reductions in soil bulk density (Harris, 1967). Soil bulk density converges in the vegetation types at 30-50 cm, coinciding with the deepest observed rooting depth of GL roots (Figures 2.5 and 2.6A). We have

also observed greater gopher activity in GL at our site, with noticeable burrows and disturbed soil, compared with rare evidence of activity in CSS. The burrowing activity may contribute to lower bulk density in GL and may also create a more homogeneous soil environment due to frequent disturbance and mixing.

Soil bulk density is known to impact soil hydrology and plant root growth, with less dense soils promoting faster water infiltration and greater root growth (Meek et al., 1992), meaning precipitation may more easily infiltrate the surface soil in GL, where it is quickly taken up by the large webs of fine roots. In contrast, CSS likely has a slower infiltration rate, which may lead to more runoff, as the precipitation is not easily absorbed by the dense soils. A previous study from our site indicates that utilizing hydrology models from similar shrub/grassland boundaries in the American Southwest proposed that runoff from shrub areas may be funneled to nearby grasslands, further promoting stable mosaics of shrub- and grasslands (Mueller et al., 2007). The denser soils in CSS may also act as a barrier to grass invasion as herbaceous grass seedling roots may not be able to penetrate (Harris, 1967; USDA NRCS, 2008; Hillel, 2004). The differences in soil bulk density between vegetation types may provide evidence of vegetation specific plant-soil feedbacks that reinforce the ongoing boundary stability, where soil and hydrological conditions favor the current vegetation type and prevent invasion from vegetation with differing rooting or water-use strategies.

The trends in SOC and N content and distribution also appear to be linked to differences in vegetation properties in both vegetation types. CSS had greater SOC at the surface (0-20 cm), and below 50 cm (Figures 6B and 6C). Several studies have found that shrub litter is high in recalcitrant SOC, such as phenols and lignin (Gray and Schlesinger, 1981; Westman and Oleary, 1986; Blank, 2008; Wolkovich et al., 2010; Dickens and Allen, 2014), and has lower

decomposability than herbaceous grass litter that leads to greater SOC sequestration near the surface in shrublands (Cable et al., 2009; Montane et al., 2010; Dickens and Allen, 2013). CSS also exhibited greater SOC and N content beyond 100 cm depth, which we believe is directly related to the greater root biomass in CSS beyond 50 cm (Figures 2.5A, 2.6C, and 2.6G). The heterogeneous distribution of soil resources in CSS may also play a role in preventing GL invasion of CSS, and previous studies have proposed that shrubs create "islands of fertility" that concentrate soil resources directly below shrub canopies, preventing invasion of the bare areas in shrublands (Schlesinger et al., 1996; Schelsinger and Pilmanis, 1998; Bird et al., 2000).

The C/N ratio was greater at the surface in CSS, which may be attributed to the greater amounts of SOC or may be an indicator of differing belowground biotic communities and/or decomposition rates (Figure 2.6E). Soil C/N ratio is often used as an indicator of soil health (Xu et al., 2016) and greater C/N ratios generally result in slower decomposition (Brady and Weil, 2002; Xu et al., 2016). Several studies have demonstrated that belowground biotic communities are highly specific to aboveground vegetation type (Bardgett and Wardle, 2010; van der Putten et al., 2013), and previous research from our study site confirms that CSS and GL had unique surface microbial communities (Khalili et al., 2016; Finks et al., 2021).

Implications of the stable boundary

Our results indicate that the adjacent CSS and GL vegetation types exist on similar physical conditions at our site. The documented boundary stability across the available timeline despite frequent wildfire and historic drought conditions is consistent with the interpretation that the two habitats are alternative stable states (Laycock, 1991; Mueller et al., 2007). The differences found in soil properties across the boundary in relation to vegetation type likely act as factors of

ecological resistance, further reinforcing the stable boundary and preventing expansion of either species. Theories of alternative stable state suggest that the two vegetation types will remain stable unless some drastic perturbation forces the ecosystem across a threshold of stability, yielding a competitive advantage to one species that allows them to overtake the other (Laycock, 1991). Studies have proposed that increased fire frequency, drought, and N deposition, especially when combined, will lead to grass invasion of shrublands (Laycock, 1991, Talluto and Suding, 2008, Kimball et al., 2014). As all three of these factors are predicted to increase in the near future (Fenn et al., 1998; Seager and Vecchi,, 2010; Cayan et al., 2010), quantifying and understanding the relative contribution of each factor to the perturbation of the stable states will be an important aspect of predicting ecosystem function and dynamics in shrub- and grasslands in the future.

2.7 References

Bardgett, R. D., & Wardle, D. A. (2010). *Aboveground-belowground linkages: biotic interactions, ecosystem processes, and global change*. Oxford University Press.

Bird, S. B., Herrick, J. E., Wander, M. M., & Wright, S. F. (2002). Spatial heterogeneity of aggregate stability and soil carbon in semi-arid rangeland. *Environmental Pollution*, *116*(3), 445-455.

Biswell, H. H. H. (1956). Ecology of California grasslands. *Rangeland Ecology & Management/Journal of Range Management Archives*, *9*(1), 19-24.

Blank, R. R. (2008). Biogeochemistry of plant invasion: a case study with downy brome (Bromus tectorum). *Invasive Plant Science and Management*, *1*(2), 226-238.

Brady, N. C., & Weil, R. R. (2002). Soil and the hydrologic cycle. *The Nature and Properties of Soils*, 2.

Cable, J. M., Ogle, K., Tyler, A. P., Pavao-Zuckerman, M. A., & Huxman, T. E. (2009). Woody plant encroachment impacts on soil carbon and microbial processes: results from a hierarchical Bayesian analysis of soil incubation data. *Plant and Soil, 320*(1), 153-167.

Cayan, D. R., Das, T., Pierce, D. W., Barnett, T. P., Tyree, M., & Gershunov, A. (2010). Future dryness in the southwest US and the hydrology of the early 21st century drought. *Proceedings of the National Academy of Sciences*, *107*(50), 21271-21276.

Cleland, E. E., Funk, J. L., & Allen, E. B. (2016). Coastal Sage Scrub. In *Ecosystems of california* (pp. 429-448). University of California Press.

D'Antonio, C. M., & Vitousek, P. M. (1992). Biological invasions by exotic grasses, the grass/fire cycle, and global change. *Annual review of ecology and systematics*, *23*(1), 63-87.

Davis, S.D. and Mooney, H.A. (1985) Comparative water relations of adjacent California shrub and grassland communities. Oecologia 66: 522-529.

Dickens, S.J.M., Allen, E.B. (2014) Exotic plant invasion alters chaparral ecosystem resistance and resilience pre- and post-wildfire. *Biol Invasions* 16, 1119–1130.

Fenn, M. E., Poth, M. A., Aber, J. D., Baron, J. S., Bormann, B. T., Johnson, D. W., ... & Stottlemyer, R. (1998). Nitrogen excess in North American ecosystems: predisposing factors, ecosystem responses, and management strategies. *Ecological Applications, 8*(3), 706-733.

Finks, S. S., Weihe, C., Kimball, S., Allison, S. D., Martiny, A. C., Treseder, K. K., & Martiny, J. B. (2021). Microbial community response to a decade of simulated global changes depends on the plant community. *Elementa: Science of the Anthropocene, 9*(1).

Germino, M. J., Belnap, J., Stark, J. M., Allen, E. B., & Rau, B. M. (2016). Ecosystem impacts of exotic annual invaders in the genus Bromus. In *Exotic brome-grasses in arid and semiarid ecosystems of the Western US* (pp. 61-95). Springer, Cham.

Gray, J. T., & Schlesinger, W. H. (1981). Nutrient cycling in Mediterranean type ecosystems. *Resource use by chaparral and matorral*, 259-285.

Harris, G.A. (1967), Some Competitive Relationships between Agropyron spicatum and Bromus tectorum. Ecological Monographs, 37: 89-111.

Hendry, G. W. (1931). The Adobe brick as a historical source: reporting further studies in adobe brick analysis. *Agricultural History*, *5*(3), 110-127.

Hillel, D. (2004) Introduction to environmental soil physics. Elsevier, Amsterdam

Hobbs, E. R. (1983). *Factors controlling the form and location of the boundary between coastal sage scrub and grassland in southern California* (Doctoral dissertation, University of California, Los Angeles).

Jackson, R. B., H. J. Schenk, E. G. Jobbágy, J. Canadell, G. D. Colello, R. E. Dickinson, C. B. Field, P. Friedlingstein, M. Heimann, K. Hibbard, D. W. Kicklighter, A. Kleidon, R. P. Neilson, W. J. Parton, O. E. Sala, and M. T. Sykes. (2000). Belowground consequences of vegetation change and their treatment in models. *Ecological Applications* 10: 470– 483.

Jenny, H. (1941). Factors of soil formation. McGraw-Hill, New York. *Factors of soil formation. McGraw-Hill, New York.*

Jenny, H. (1958). Role of the plant factor in the pedogenic functions. *Ecology*, *39*(1), 5-16.

Jenny, H. (1994). *Factors of soil formation: a system of quantitative pedology*. Courier Corporation.

Jobbágy, E. G., & Jackson, R. B. (2000). The vertical distribution of soil organic carbon and its relation to climate and vegetation. *Ecological applications*, *10*(2), 423-436.

Khalili, B., Ogunseitan, O., Goulden, M.L., Allison, S.D. (2016) Interactive effects of precipitation manipulation and nitrogen addition on soil properties in California grassland and shrubland,Applied Soil Ecology, Volume 107, Pages 144-153.

Kimball, S., Goulden, M.L., Suding, K.N. and Parker, S. (2014), Altered water and nitrogen input shifts succession in a southern California coastal sage community. Ecological Applications, 24: 1390-1404.

Laycock, W.A. (1989). Secondary succession and range condition criteria: Introduction to the problem. p. l-15. In: W.K. Lauenroth and W.A. Laycock, (eds). Secondary succession and the evaluation of rangeland condition. Westview Press, Boulder, Colo.

Laycock, W. A. (1991). Stable states and thresholds of range condition on North American rangelands: a viewpoint. *Rangeland Ecology & Management/Journal of Range Management Archives*, *44*(5), 427-433.

Meek, B. D., Rechel, E. R., Carter, L. M., DeTar, W. R., & Urie, A. L. (1992). Infiltration rate of a sandy loam soil: effects of traffic, tillage, and plant roots. *Soil Science Society of America Journal*, *56*(3), 908-913.

Montané, F., Romanyà, J., Rovira, P., & Casals, P. (2010). Aboveground litter quality changes may drive soil organic carbon increase after shrub encroachment into mountain grasslands. *Plant and Soil*, *337*(1), 151-165.

Mooney, H. A., Hamburg, S. P., & Drake, J. A. (1986). The invasions of plants and animals into California. In *Ecology of biological invasions of North America and Hawaii* (pp. 250-272). Springer, New York, NY.

Mooney, H. A., & Hobbs, R. J. (2000). Global change and invasive species: where do we go from here. *Invasive species in a changing world. Island Press, Washington, DC*, 425-434.

Mueller, E. N., Wainwright, J., & Parsons, A. J. (2007). The stability of vegetation boundaries and the propagation of desertification in the American Southwest: A modelling approach. *Ecological Modelling*, *208*(2-4), 91-101.

Noss, R.F.; Laroei, E.T.; Scott, J.M. (1995). Endangered ecosystems of the United States: A preliminary assessment of loss and degradation. Biological Report 28. US National Biological Service, Washington, DC. Available at: http://biology.usgs.gov/pubs/ecosys.htm

Pasquini, S. (2008). Vegetation responses to anthropogenic nitrogen deposition and nitrogen fertilization in chaparral and coastal sage scrub of Southern California. Master's Thesis, California State University San Marcos.

Parker, S. (2019). Climate and plant resource controls on coastal sage scrub ecohydrology and succession. Doctoral Dissertation, University of California Irvine

Potts, D.L., Suding, K.N., Winston, G.C., Rocha, A.V., Goulden, M.L. (2012). Ecological effects of experimental drought and prescribed fire in a southern California coastal grassland, J. Arid Environ., 81, pp. 59-66

Schlesinger, W. H., & Pilmanis, A. M. (1998). Plant-soil interactions in deserts. *Biogeochemistry*, *42*(1), 169-187.

Schlesinger, W. H., Raikes, J. A., Hartley, A. E., & Cross, A. F. (1996). On the spatial pattern of soil nutrients in desert ecosystems: ecological archives E077-002. *Ecology*, *77*(2), 364-374.

Schultz, A.M., Launchbaugh, J.L., Biswell, H.H. (1955). Relationship between grass density and brush seedling survival. Ecology 36:226–238

Seager, R., & Vecchi, G. A. (2010). Greenhouse warming and the 21st century hydroclimate of southwestern North America. *Proceedings of the National Academy of Sciences*, *107*(50), 21277-21282.

Talluto, M.V., Suding, K.N. (2008). Historical change in coastal sage scrub in southern California, USA in relation to fire frequency and air pollution. *Landscape Ecol* 23, 803–815.

USDA National Resources Conservation Service. (2008). Soil quality indicators. [Fact Sheet]

van der Putten, W.H., Bardgett, R.D., Bever, J.D., Bezemer, T.M., Casper, B.B., Fukami, T., Kardol, P., Klironomos, J.N., Kulmatiski, A., Schweitzer, J.A., Suding, K.N., Van de Voorde, T.F.J. and Wardle, D.A. (2013), Plant–soil feedbacks: the past, the present and future challenges. J Ecol, 101: 265-276.

Vitousek, P. M., D'antonio, C. M., Loope, L. L., Rejmanek, M., & Westbrooks, R. (1997). Introduced species: a significant component of human-caused global change. *New Zealand Journal of Ecology*, 1-16.

Veneklaas, E. & Poot, P. (2003). Seasonal patterns in water use and leaf turnover of different plant functional types in a species-rich woodland, South-western Australia. Plant and Soil. 257. 295–304. 10.1023/A:1027383920150.

Westman, W. E., & O'Leary, J. F. (1986). Measures of resilience: the response of coastal sage scrub to fire. *Vegetation*, *65*(3), 179-189.

Westoby, M., B. Walker, and I. Noy-Meir. (1989). Opportunistic management for rangelands not at equilibrium. J. Range Manage. 42266-274.

Wolkovich, E. M., Lipson, D. A., Virginia, R. A., Cottingham, K. L., & Bolger, D. T. (2010). Grass invasion causes rapid increases in ecosystem carbon and nitrogen storage in a semiarid shrubland. *Global Change Biology*, *16*(4), 1351-1365.

Xu, X., Shi, Z., Li, D., Rey, A., Ruan, H., Craine, J. M., ... & Luo, Y. (2016). Soil properties control decomposition of soil organic carbon: Results from data-assimilation analysis. *Geoderma*, *262*, 235-242.

Chapter 3.

Drought induced vegetation shifts from shrub to grassland impact above and belowground properties

3.1 Abstract

We conducted a long-term, large-scale, multi-factorial rainfall and nitrogen (N) manipulation experiment in adjacent Mediterranean coastal sage scrub (CSS) and annual, invasive grassland (GL) habitats in southern California to evaluate the effects of 13 years of drought and added N on above- and belowground properties. We found that response to manipulations depended on vegetation type, with CSS showing greater sensitivity to the treatments than nearby GL. In CSS, drought and drought × +N decreased native shrub biomass by 68% and 69%, respectively. This led to shifts in litter composition, with reduced shrub litter and an accumulation of grass litter, reflecting increased invasion by GL. Drought and drought × +N led to reductions in soil bulk density, soil organic carbon, and C/N ratio in the surface soil in CSS plots. The surface soil properties in the CSS drought plots were statistically more similar to GL than to CSS, indicating that vegetation shifts from CSS to GL impact soil properties and processes. We identified drought as the main driver of conversion from CSS to GL and conclude that the widespread invasion and loss of CSS habitats statewide may have important implications for ecosystem structure and function, both above- and belowground.

3.2 Introduction

Coastal sage scrub (CSS) is a fire-adapted and drought deciduous ecosystem that is known for high species diversity and endemism and is considered one of the most endangered ecosystem types in the United States (Noss et al., 1995). CSS historically occupied the Pacific coastal ranges from Baja California Norte in Mexico to the San Francisco Bay area in California (Holland and Keil, 1995), but studies estimate that CSS habitats have been reduced to as little as 10% of their historical extent (Rundel, 2007; Talluto and Suding, 2008). Land use change, drought, increasing fire frequency, nitrogen (N) deposition and species invasions have all been cited as drivers of CSS habitat loss (Talluto and Suding, 2008; Kimball et al., 2014).

Global change predictions for Southern California indicate reductions in precipitation, with drier winters and more severe summer droughts, more frequent and intense fires, and increases in nitrogen (N) deposition from fossil fuel sources (Seager and Vecchi, 2010; Cayan et al., 2010). The current rates of N deposition attributable to fossil fuel burning in the South Coast Air basin (including Orange, Los Angeles, Riverside and San Bernardino counties in California) are among the highest in the United States (Fenn et al. 1998, 2002). These predicted global change drivers can impact plant productivity, plant community composition, and the quantity and quality of plant derived inputs to soil, with implications for biogeochemical processes and nutrient cycling (Allison et al., 2013; Khalili et al., 2016). In this study, we focus on drought and nitrogen deposition, which in combination, are known to interact with CSS ecosystem vulnerability, triggering widespread invasion by annual, non-native grasses (Kimball et al., 2014).

Previous studies have identified invasion by annual, non-native grasses, namely species from the genera *Bromus* and *Avena,* as the primary threat to CSS (Freudenberger et al., 1987;

Minnich and Dezzani, 1998). Talluto and Suding (2008) estimated that 49% of the area previously covered by CSS had been converted to invasive Eurasian grassland between 1930 and 2005, and only 15% remained uninvaded. These conversions from CSS to GL not only lead to losses of native, endemic habitats, but also cause alterations in ecosystem structure and function both above- and belowground (D'Antonio and Vitousek, 1992; Wood et al., 2006).

Here, we took advantage of a long-term field experiment to examine how experimental rainfall reduction and nitrogen (N) addition impact above- and belowground ecosystem properties in adjacent CSS and GL habitats at the Loma Ridge Global Change Experiment (LRGCE). The LRGCE explores the impacts of precipitation change (ambient or reduced (drought)) and nitrogen addition (ambient or +N) in CSS and GL habitats along a vegetation boundary that has been stable since at least 1939. Previous work at LRGCE focused on the impacts of both drought and nitrogen deposition on aboveground vegetation in CSS and GL and found that the drought and drought × +N treatments decreased native shrub cover and increased the cover of invasive grasses in CSS during early succession (Kimball et al., 2014). Our analyses explored both the long-term, and combined effects of drought and nitrogen addition on these habitats, with a particular focus on treatment impacts belowground. We incorporated soil sampling to two meters depth to more fully quantify changes in root biomass and soil properties. Mechanistic understanding of how soils respond to drought, nitrogen addition, and the associated vegetation shifts is required to accurately predict how the terrestrial carbon pool will respond to global change.

We focused on the following questions: 1.) How do long-term drought and added nitrogen impact aboveground vegetation along a stable boundary between CSS and GL?; 2.) How do belowground vegetation and soil properties respond to drought and added nitrogen? 3.) Do changes in aboveground vegetation correlate with changes belowground? 4.) Does the vegetation shift from

CSS to GL impact belowground properties?

3.3 Methods

Study site

All data were collected in Spring 2020 in plots at the LRGCE located on a gentle, northwest facing slope at the foothills of the Santa Ana Mountains (117.704 W, 33.742 N). The plots experience a Mediterranean climate, characterized by warm, dry summers and mild, wet winters. The annual average high temperature is 24.1 ℃ and the annual average low is 9.7 ℃. The mean precipitation is 327 mm per year, and generally falls in the months of November-April. The LRGCE started in 2006 and uses factorial manipulations of precipitation and nitrogen to examine the effects of global change on adjacent Mediterranean CSS and GL plots. The experiment uses a randomized, split plot design with eight replicate blocks in each vegetation type. Each replicate block contains three plots, one with each of the three precipitation levels: ambient, added (+40%), and drought (-40%). Our analyses focused only on the ambient and drought manipulations (Figure 3.1). Precipitation was reduced through the installation of retractable polyethylene roofs that were closed during approximately half of the rain events (closed <5% of the days during a year) (Figure 3.2). The plots were split lengthwise, and one side was randomly selected to receive added nitrogen. Added nitrogen (+N) plots received 2 g N m^2 calcium nitrate prior to the first rain of the growing season and 4 g N m^2 100-day calcium nitrate shortly after the onset of the growing season (Parolari et al., 2012). LRGCE currently receives approximately 1.5 g N m^{-2} yr^{-1} from nitrogen deposition (Fenn et al., 2010), thus the added nitrogen plots simulate high levels of nitrogen deposition (Kimball et al., 2014).

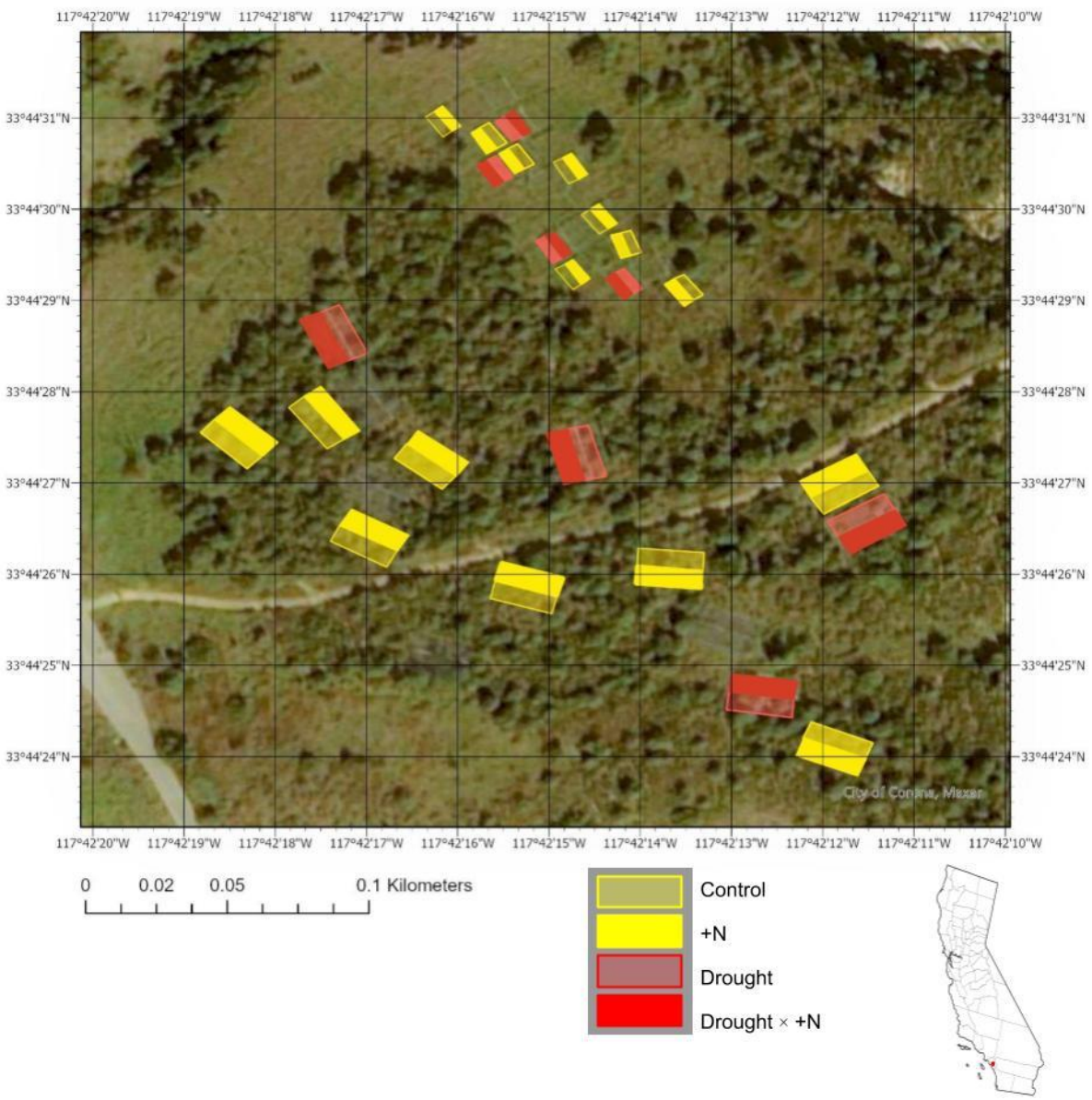

Figure 3.1. Study site and experimental design at the Loma Ridge Global Change Experiment in Irvine, California, color coded by precipitation treatment (control or drought), and nitrogen treatment (control, added (+N)).

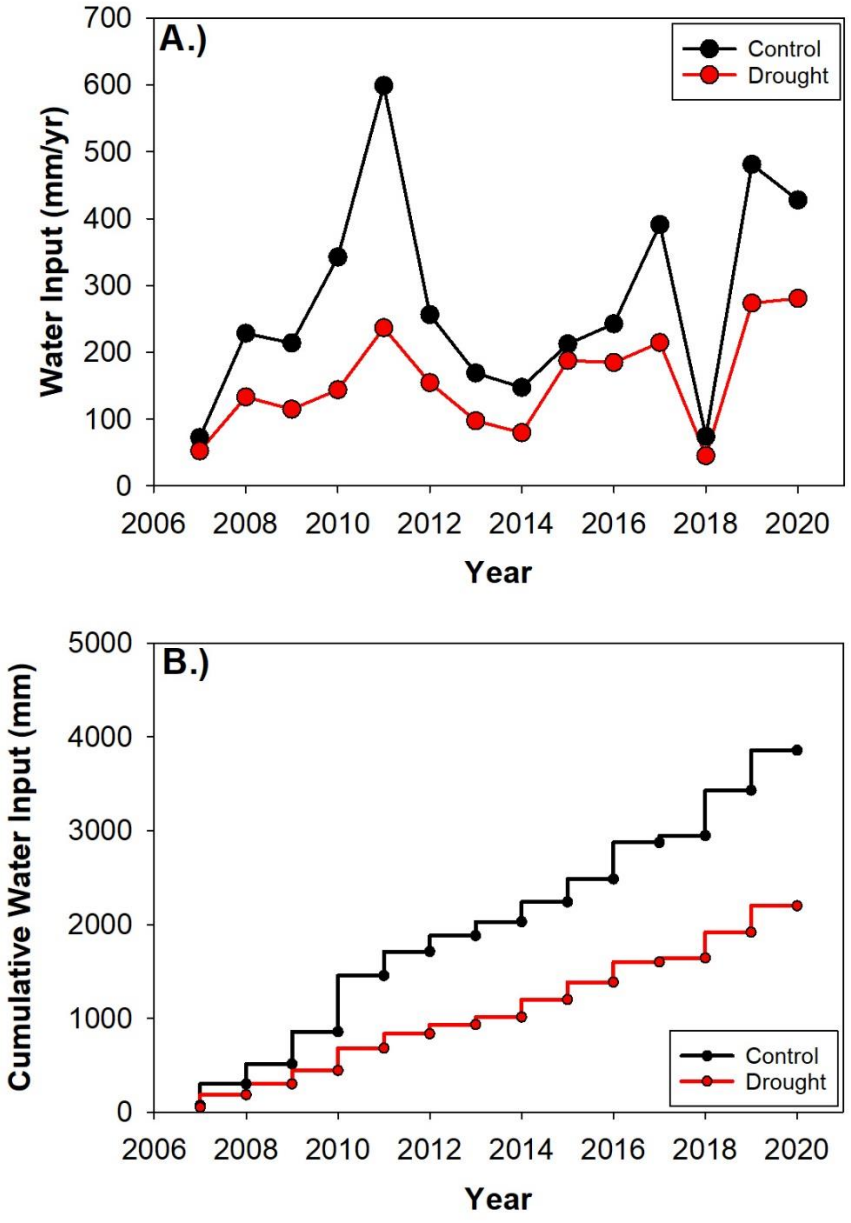

Figure 3.2. A.) Annual and B.) cumulative water input by year and treatment at the Loma Ridge Global Change Experiment.

Vegetation cover and composition

We measured fractional species composition and cover during peak growing season (March 2020). In CSS, species composition and cover were measured as fractional cover by species over the total area in each plot. In GL, species composition and cover were measured by point intercept method, using two 160 × 60 cm^2 polyvinyl chloride frames with 10 cm interval grids positioned in each plot. The first-intercepted species at each interval point was recorded, and if no species were found, the point was recorded as litter or bare soil. The number of interceptions for each species was then summed within each plot to calculate fractional cover.

Vegetation live biomass and litter pools

Live herbaceous biomass and litter were collected from each plot. Four 14 cm by 50 cm polyvinyl chloride frames were harvested and sorted by type (grass or forb). Litter was also collected within each frame and was sorted by type: grass litter, or leaf litter and coarse woody debris. All biomass and litter samples were returned to the lab, dried at 65℃ for 4 days, and weighed.

The volume of all individual shrubs within a four by four meter center subplot was calculated in CSS plots using measurements of height, and two perpendicular width measurements, assuming a spherical shape. Shrub volume was then converted to biomass using species specific volume-mass relationships (Pasquini 2008; Table A.6).

Soil Core Sampling

One soil core to two meters depth was taken at a randomly selected location within each plot using a 5.7 cm diameter soil auger (N=8 for ambient plots, N=4 for treatment plots). Each soil

core was separated by depth range (0-10 cm, 10-20 cm, 20-30 cm, 30-50 cm, 50-100 cm, 100-150 cm, and 150-200 cm). All soil cores were taken back to the lab and dried to constant mass at 105°C. Bulk density was calculated as the total mass of dry soil per volume of depth range. Soils were sieved to 2 mm and root biomass was collected from each soil core and depth range, which were then washed, dried and weighed. A subsample of sieved soil was then pulverized. An aliquot of pulverized soil assayed for elemental C and N composition on a NC Soil Analyzer 2400 (Thermofisher).

Statistical analyses

The observed above- and belowground properties were analyzed using three-way analysis of variance to examine the effects of vegetation type (CSS vs. GL), precipitation treatment (control vs. drought) and nitrogen treatment (control vs. +N), and their interactions. We performed multiple pairwise comparisons using the Tukey-Kramer method to account for the unbalanced sample sizes. We ran simple linear regressions between each belowground property and corresponding above or belowground property measured to examine the drivers of belowground changes.

3.4 Results

The above- and belowground properties measured in this study showed no significant three-way interactions between vegetation type, rainfall treatments, and nitrogen treatments. Most properties displayed significant main effects due to vegetation type and rainfall treatment, and interaction effects between vegetation type and rainfall treatment, and occasional properties displayed significant interactions between rainfall and nitrogen treatments. The differences found between vegetation types (CSS vs. GL) were often larger than those found between treatments. Within each vegetation type, rainfall treatment was often the most significant driver of change.

GL response to treatments

GL showed no significant response to treatments neither above- nor belowground, aside from the +N treatment having significantly higher soil N at 20-30 cm than the drought × +N treatment (Figures A.1, A.2, A.3). While changes in GL properties in response to treatment were notable, particularly aboveground, the small magnitude of the changes combined with high variability led to little statistical significance. Overall, CSS properties were generally more sensitive to the treatments than GL properties, and we therefore will focus mainly on the impacts of treatments in CSS.

CSS response to treatments

Within the CSS treatments, drought was the main driver of change. N addition showed little statistical impact overall, although occasional interactions between rainfall treatment and N treatment were observed, indicating that N addition may impact CSS when combined with drought.

CSS aboveground biomass and litter

The drought and drought × +N treatments reduced live shrub biomass by -68% ($p=0.0467$**)** and -69% ($p=0.1424$) respectively, while herbaceous grass and forb biomass showed little change (Figure 3.3). There was a shift in litter composition in both drought treatments, with notable decreases in shrub leaf litter and coarse woody debris (fallen dead shrub stems and branches) and increases in the amount of grass litter. The drought, ambient N treatment displayed significant increases in the mass of standing dead shrubs (still rooted in soil) when compared to the control ($p=0.0096$). In both drought treatments the mass of dead material was greater than the mass of live material (Figure 3.3). The + N treatment showed no change in aboveground biomass nor litter

(Figure 3.3). Overall, both drought treatments displayed widespread shrub die-off and an accumulation of grass litter.

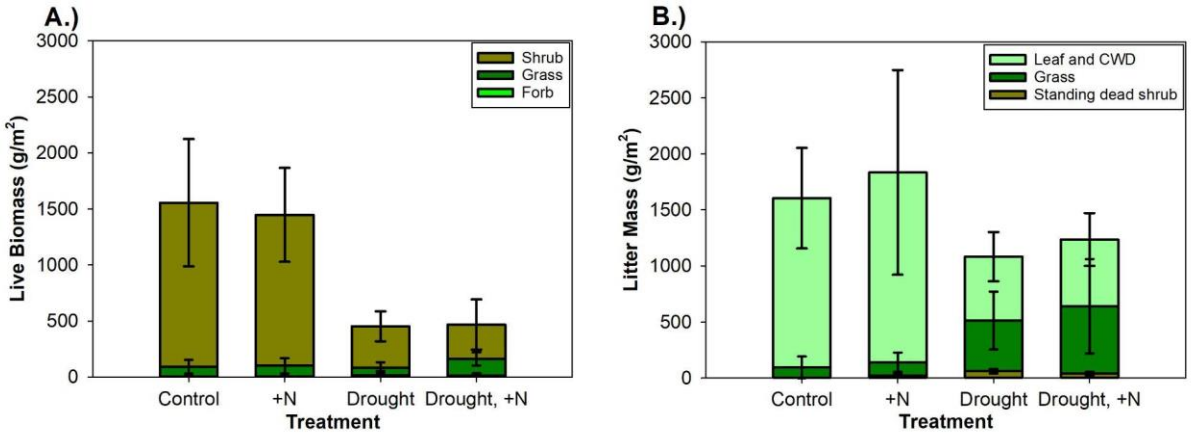

Figure 3.3. A.) Live biomass and B.) litter mass pools in Coastal Sage Scrub at the Loma Ridge Global Change Experiment. Error bars indicate standard error.

CSS root biomass

Root biomass was highly variable across vegetation types and treatments, but in CSS there were notable reductions in root biomass in both drought treatments. Although not statistically significant, drought and drought × +N treatments displayed 43% (p=0.4923) and 54% (p=0.2281) reductions in total root biomass to two meters depth respectively. The +N treatment showed no change in root biomass at any depth, nor in total root biomass (Figure 3.4A).

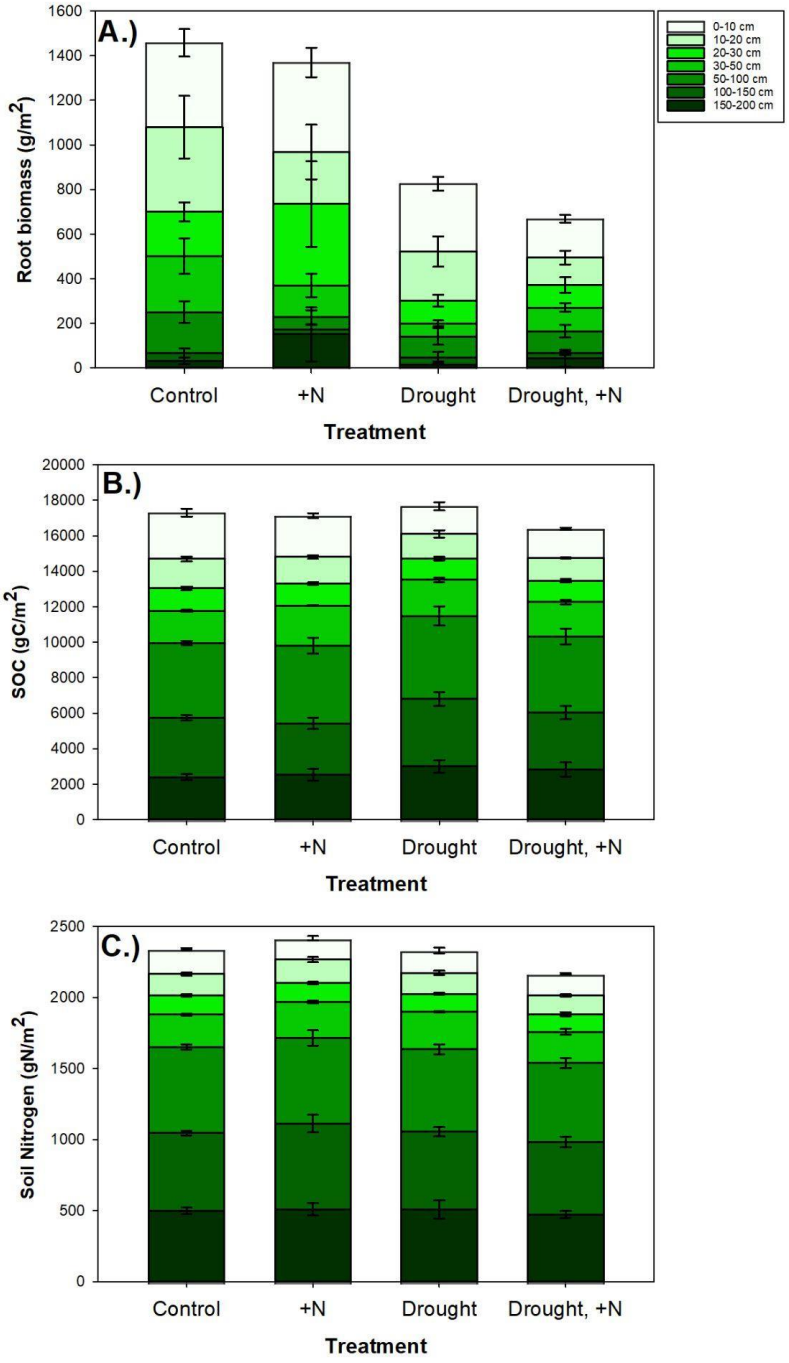

Figure 3.4. Root biomass, soil organic carbon, and soil nitrogen stocks in Coastal Sage Scrub habitat at the Loma Ridge Global Change Experiment. Error bars indicate standard error. A.) Root biomass B.) soil organic carbon stocks, and C.) soil nitrogen stocks by depth layer in each treatment.

CSS bulk density

The drought and drought × +N treatments led to a 16% (p=0.0145) and 14% (p=0.0556) decrease in soil bulk density at the surface (0-10 cm) respectively. The +N treatment showed no change (Figure 3.5A). Bulk density was negatively correlated with the amount of grass litter in CSS (r^2=0.193; p=0.05) (Figure 3.6).

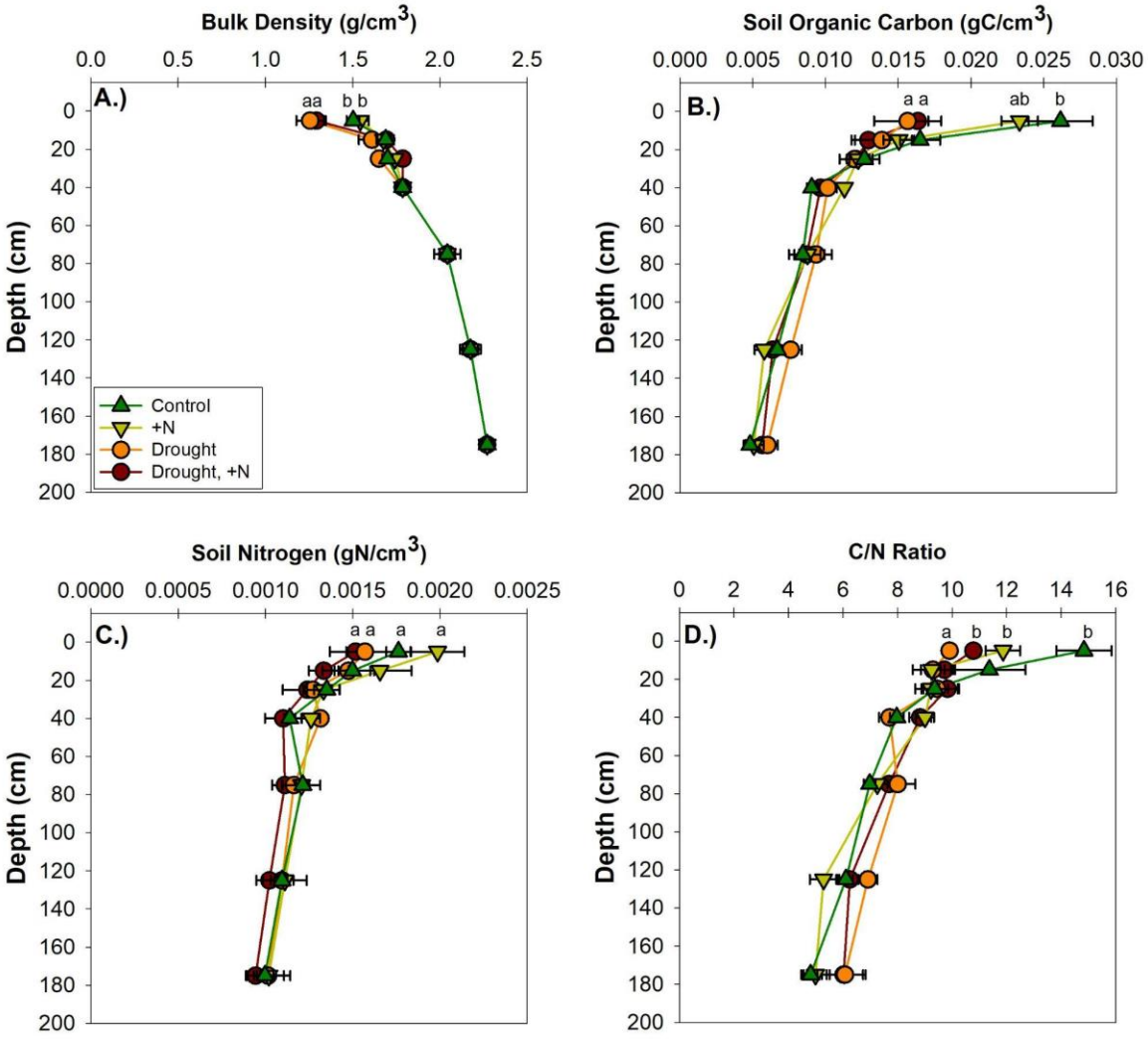

Figure 3.5. Soil properties by depth in Coastal Sage Scrub at the Loma Ridge Global Change Experiment. Error bars represent standard error. Treatments marked with different letters indicate statistical difference (p<0.05) in 0-10 cm depth. No statistical differences were found below 0-10 cm. A.) Bulk density, B.) organic carbon, C.) nitrogen, and D.) C/N ratio by depth in each treatment.

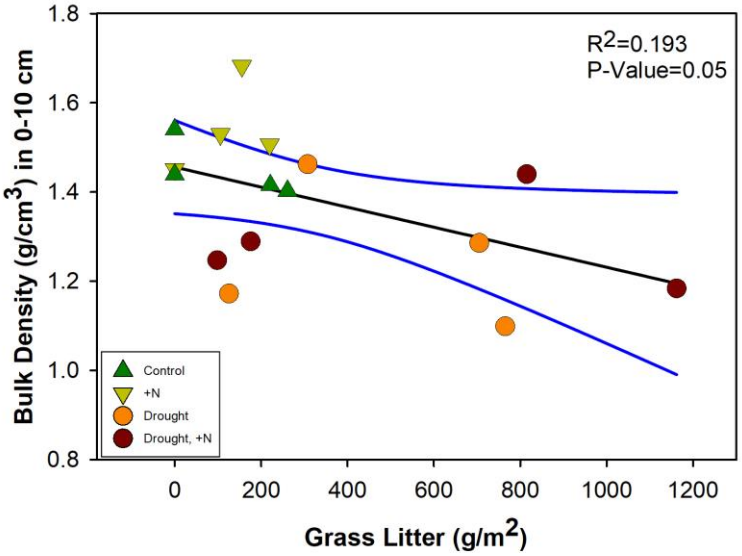

Figure 3.6. Correlation between aboveground grass litter mass and soil bulk density at 0-10 cm depth in Coastal Sage Scrub habitat at the Loma Ridge Global Change Experiment. Black line indicates line of best fit, and blue lines indicate 95% confidence interval.

CSS soil organic carbon

Drought and drought × +N treatments displayed -40% (p=0.0008) and -32% (p=0.002) reductions in soil organic carbon (SOC) (gC/cm^3) at the surface (0-10 cm) (Figure 3.5B). SOC below 10 cm was unaffected. The + N treatment showed no change at any depth compared to the control. Despite large reductions near the surface in both drought treatments, total SOC stocks to two meters were not significantly different from the control (Figure 3.4B). We found that SOC was positively correlated with root biomass in 0-10 cm (r^2=0.378; p=0.002) and 10-20 cm (r^2=0.340; p=0.004) in CSS (Figure 3.7).

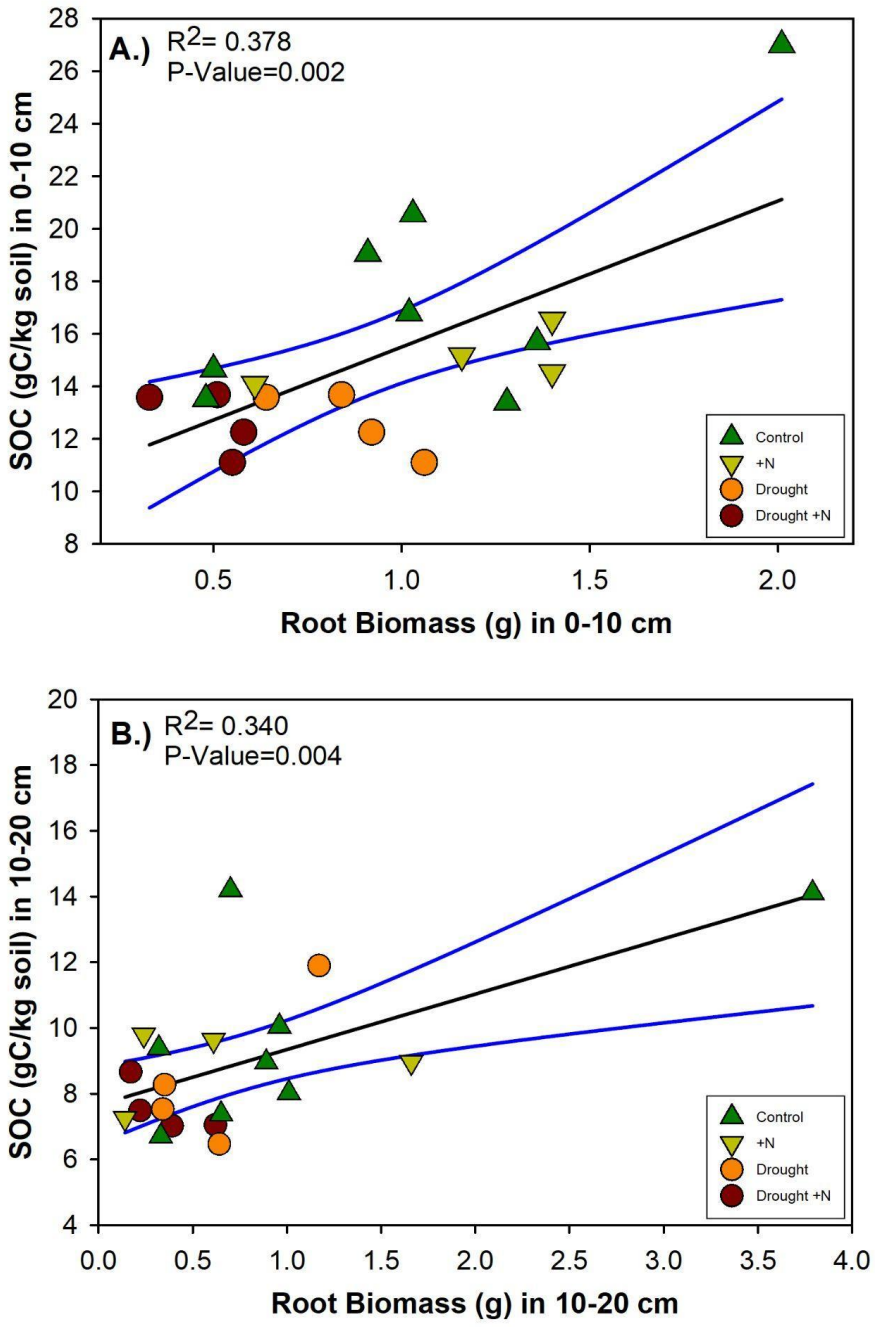

Figure 3.7. Correlations between root biomass and soil organic carbon (SOC) content in A.) 0-10 and B.) 10-20 cm in Coastal Sage Scrub habitat found at the Loma Ridge Global Change Experiment. Black line indicates line of best fit, and blue lines indicate 95% confidence interval.

CSS soil N and C/N ratio

Despite yearly N additions of 6 gN/m^2, there were no significant trends in soil N in response to treatments in CSS (Figures 3.4C and 3.5C). Both drought treatments displayed decreases in the C/N ratio at the surface (0-10 cm). Drought displayed a 33% decrease ($p=0.0486$), and combined drought × +N displayed a 27% decrease ($p=0.4461$) in C/N ratio compared to the control. The +N treatment showed no significant change at any depth.

Drought induced shifts from CSS to GL

The drought and drought × +N treatments in CSS displayed widespread native shrub die off, increases in standing dead shrub mass, and shifts in litter composition that demonstrate grass litter accumulation, and losses of shrub litter. These changes aboveground were mirrored in the surface soil, and led to reductions in soil bulk density, SOC, and in the C/N ratio of the soil. Surface (0-10 cm) soil bulk density, SOC, and C/N ratio in the CSS drought treatments were statistically more similar to the GL control than the CSS control (Figure 3.8). Only soil N remained more similar to the CSS control than GL. We found significant correlations that indicate greater grass litter led to reductions in surface soil bulk density in CSS (Figure 3.6), and that the loss of root biomass in CSS drought treatments correlated with lower SOC in 0-10 cm and 10-20 cm (Figure 3.7). Overall, drought caused a vegetation shift from CSS to GL that was visible in both above and belowground properties.

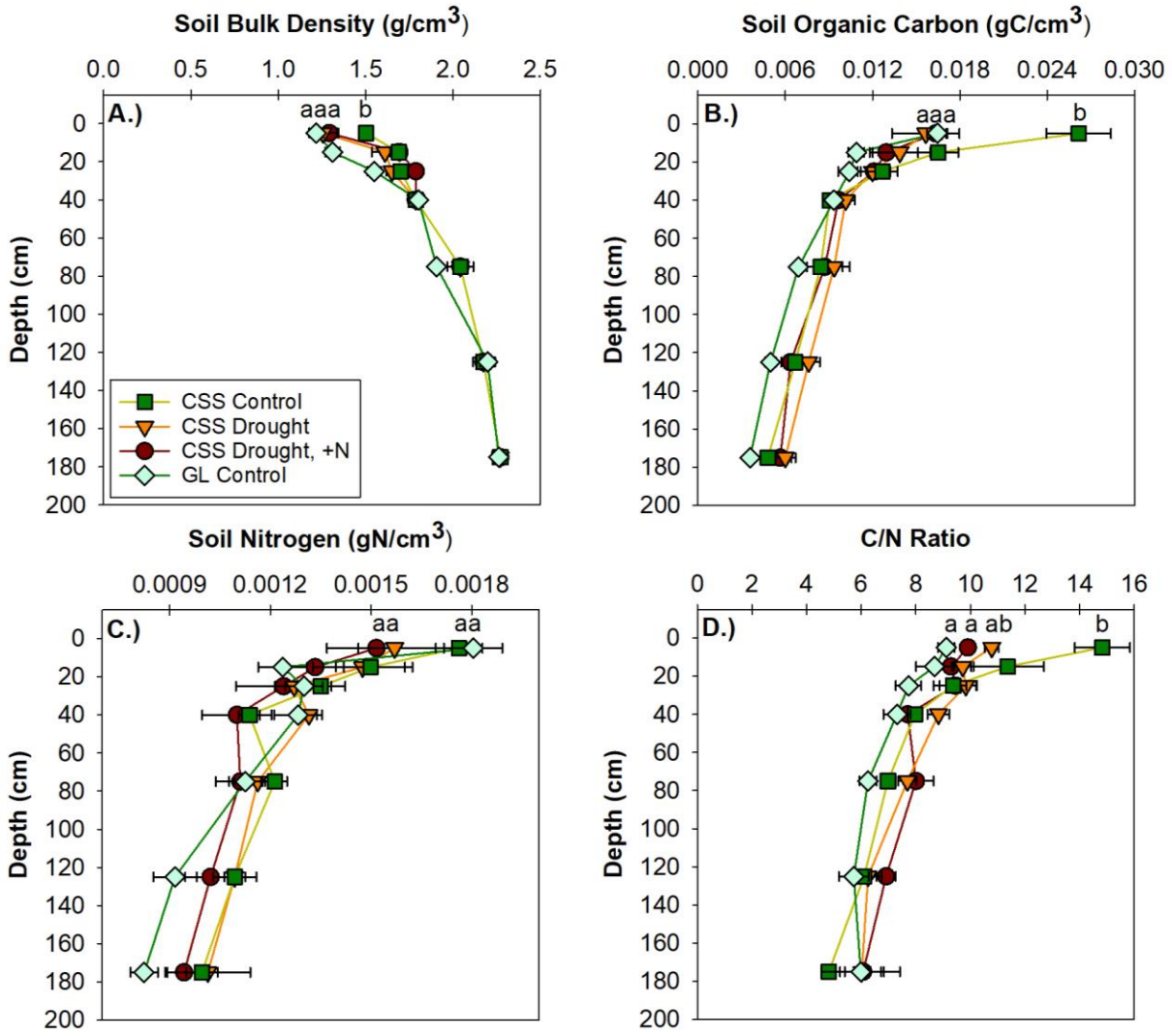

Figure 3.8. Drought induced shifts from Coastal Sage Scrub (CSS) to Grassland (GL) in the CSS habitat found at the Loma Ridge Global Change Experiment. Error bars represent standard error of the mean. Treatments marked with different letters indicate statistical difference ($p<0.05$) in 0-10 cm depth. No statistical differences were found below 0-10 cm. A.) Similarities in surface soil bulk density in CSS drought plots and GL. B.) Similarities in surface soil organic carbon in CSS drought plots and GL. C.) No change in soil nitrogen in CSS drought plots. D.) Similarities in surface soil C/N ratio in CSS drought plots and GL.

3.5 Discussion

Rapid shifts in aboveground vegetation in response to treatments

Consistent with previous studies, drought and drought × +N caused reductions in native shrub biomass and triggered a vegetation shift from CSS toward GL (Kimball et al., 2014). In our study, N addition (+N) alone did not cause shrub die-back nor grass invasion, indicating that drought was the main driver of this conversion. Extended drought likely caused openings in the shrub canopy, enabling fast-growing, non-native grasses to invade. Previous studies have documented that shrub canopy openings caused by drought, fire, or other disturbance allow the space for grass invasion, which then are able to quickly access excess N, leading to greater invasive proliferation when combined with N enrichment (Seabloom et al., 2003; Gea-Izquierdo et al., 2007; Jiménez et al., 2011; Diez et al., 2012; Kimball et al., 2014). While we did not find significant differences between drought and combined drought × + N treatments in the CSS plots, a previous study at our site identified that combined drought × + N treatments had higher instances of grass invasion (Kimball et al., 2014).

Despite long-term rainfall reductions and N additions, GL showed no significant responses to treatments in this study. The annual growth pattern and high ecological resilience of GL largely explain the lack of response, particularly in the soil measurements. Previous research at our site indicates that GL biomass responds nearly linearly with increasing precipitation, until saturating around 250 mm per year (Parolari et al., 2015), which means that drought plots experienced similar growth and biomass density as control plots in years of precipitation greater than 250 mm. Both the year data was collected and the year prior experienced precipitation greater than 250 mm (Figure 3.2), thus the lack of treatment response in GL aboveground is expected. Belowground

measurements such as bulk density and C and N content would also be impacted by interannual variability in aboveground biomass, leading to a muted treatment response belowground.

Our results indicate greater sensitivity to treatments, particularly drought, in CSS. While CSS habitats are adapted to seasonal and long-term drought, they are typically found in areas of precipitation ranging from 250-500 mm per year (Harrison et al., 1971). The drought treatments received an average of 156 mm per year of water across the thirteen years studied, and nine of the years greatly exceeded the lower end of the precipitation range, particularly during the 2012-2016 drought (Figure 3.2). Ambient rainfall during the same time frame was on average 267 mm per year, signifying that our study site may be approaching the lower edge of the CSS habitat climate zone, and nearing the climate zone for arid grasslands (Whittaker, 1975). Although drought adapted, the perennial strategy of species in CSS may serve as a disadvantage in drier climates with high interannual rainfall variability climates, and especially during times of extended drought. As both the frequency and severity of drought are predicted to increase in the future (Bell et al., 2004; Griffin and Anchukaitis, 2014; Jones, 2000), we may continue to see widespread conversions of CSS to GL.

Rapid shifts belowground in response to treatment

In response to our question regarding how roots and soils respond to drought, N addition, and vegetation shifts, we found that only surface soils were sensitive to treatments, and that the changes in surface soils appeared to be associated with the vegetation shift from CSS to GL (Figure 3.8). In CSS, drought significantly reduced soil bulk density, SOC content, and C/N ratio in the surface soil, but neither total SOC nor N stocks showed change in any treatment, in neither CSS nor GL. We attribute the lack of change in SOC and N stocks to two meters to the sheer size and

known stability of these pools (Sollins et al., 1996; Schmidt et al., 2011), while the soil surface is more responsive to treatments and changes in aboveground vegetation (Minasny et al., 2017). The reductions in surface soil bulk density in CSS drought plots were correlated with higher grass litter, indicating that the invasion of grasses with shallow, dense webs of fine roots was the likely cause (Figure 3.6). The reduction in surface SOC and C/N ratio is also consistent with the transition from CSS to GL (Figure 3.8). Previous work found that grass invasion into shrublands introduced litter with less recalcitrant carbon than native shrubs, which are high in recalcitrant carbon molecules such as phenols and lignin (Gray and Schlesinger, 1981; Westman and Oleary, 1986; Blank, 2008; Wolkovich et al., 2010; Dickens and Allen, 2014). Grasses are easier to decompose than the recalcitrant shrub litter (Brady and Weil, 2002; Xu et. al., 2016), meaning grass litter would cycle at faster rates than that of the native shrubs, leading to a reduction in SOC (Dickens and Allen, 2013).

The lack of response in soil N is consistent with previous studies of fertilization in CSS and GL ecosystems, which found that added N (and other amendments) increased microbial activity and increased N immobilization, leading to no change in total N (Zink and Allen, 1998). The drought induced reduction of surface soil C/N ratio may be related to SOC loss, or may indicate changes in soil microbial communities, and/or decomposition. Soil C/N ratio is frequently used as a determinant for soil health as soil microorganisms are directly impacted by C/N ratio (Xu et. al., 2016). Greater C/N ratio generally results in slower decomposition (Brady and Weil, 2002; Xu et. al., 2016), indicating that C in CSS control plots may decompose more slowly than in both CSS drought plots and GL plots. Microbial activity is generally concentrated in the top 10 cm of soil (Brady and Weil, 2002), coinciding with the largest changes observed in this study. Previous work at our study site demonstrated that belowground biotic communities were highly

specific to vegetation type (Finks et al., 2021), which suggests that microbial communities may also be sensitive to drought induced vegetation shifts.

Implications of drought induced vegetation shifts

The vegetation shifts from CSS to GL in drought plots observed in this study have wide-reaching implications for ecosystem function and services, both above- and belowground. CSS is an endangered and endemic ecosystem that supports a great diversity of plant and animal species, over 200 of which are designated as rare, threatened, or endangered (O'Leary et al., 1992; McCaull, 1994; Bowler, 2000; Tibor, 2001). The replacement of CSS by GL threatens this unique habitat, and also causes changes in ecosystem function, such as ecosystem water balance and hydrology due to differing soil densities and rooting and water-use strategies (Davis & Mooney, 1985). The differences in biogeochemical cycling and carbon storage between the vegetation types also indicate that these vegetation shifts may have significant implications for ecosystem carbon balance. Finally, the shifts from CSS to GL have consequences for fire frequency and intensity as GL habitats are known for their high flammability and fuel load (Keeley, 1986; Minnich & Dezzani, 1998). As California heads toward a drier future, the drought induced vegetation shifts from CSS to GL have the potential to significantly alter ecosystem function and services that could further exacerbate global change. Whether the shifts from CSS to GL are reversible in years of higher rainfall will become an important factor in global change predictions in the years to come.

3.6 References

Allison, S. D., Y. Lu, C. Weihe, M. L. Goulden, A. C. Martiny, K. K. Treseder,and J. B. H. Martiny. 2013. Microbial abundance and composition influence litter decomposition response to environmental change. *Ecology* 94: 714– 725.

Bell J.L., Sloan L.C., Snyder M.A. (2004) Regional changes in extreme climatic events: a future climate scenario. J Clim 17:81–87.

Blank, R. R. (2008). Biogeochemistry of plant invasion: a case study with downy brome (Bromus tectorum). *Invasive Plant Science and Management*, *1*(2), 226-238.

Bowler, P.A. (2000) Ecological restoration of coastal sage scrub and its potential role in habitat conservation plants. *Environmental Management*, 26 (Supplement), S85–S96.

Brady, N. C., & Weil, R. R. (2008). The soils around us. *The Nature and Properties of Soils, 14th ed Pearson Prentice Hall, New Jersey and Ohio*, 1-31.

Cayan, D. R., Das, T., Pierce, D. W., Barnett, T. P., Tyree, M., & Gershunov, A. (2010). Future dryness in the southwest US and the hydrology of the early 21st century drought. *Proceedings of the National Academy of Sciences*, *107*(50), 21271-21276.

Cione, N. K., P. E. Padgett,and E. B. Allen. 2002. Restoration of a native shrubland impacted by exotic grasses, frequent fire, and nitrogen deposition in southern California. *Restoration Ecology* 10: 376–384.

D'Antonio, C. M., & Vitousek, P. M. (1992). Biological invasions by exotic grasses, the grass/fire cycle, and global change. *Annual review of ecology and systematics*, *23*(1), 63-87.

Davis, S.D., Mooney, H.A. Comparative water relations of adjacent California shrub and grassland communities. *Oecologia* **66,** 522–529 (1985).

Dickens, S.J.M., Allen, E.B. Exotic plant invasion alters chaparral ecosystem resistance and resilience pre- and post-wildfire. *Biol Invasions* **16,** 1119–1130 (2014). https://doi.org/10.1007/s10530-013-0566-0

Diez JM, D'Antonio CM, Dukes JS, Grosholz ED, Olden JD, Sorte CJ, Blumenthal DM, Bradley BA, Early R, Ibáñez I, Jones SJ, Lawler JJ, Miller LP (2012) Will extreme climatic events facilitate biological invasions? Front Ecol Env 10:249–257.

Fenn, M. E., Poth, M. A., Aber, J. D., Baron, J. S., Bormann, B. T., Johnson, D. W., ... & Stottlemyer, R. (1998). Nitrogen excess in North American ecosystems: predisposing factors, ecosystem responses, and management strategies. *Ecological Applications*, *8*(3), 706-733.

Fenn, M. E., Poth, M. A., & Arbaugh, M. J. (2002). A throughfall collection method using mixed bed ion exchange resin columns. *TheScientificWorldJOURNAL*, *2*, 122-130.

Fenn, M. E., et al . 2010. Nitrogen critical loads and management alternatives for N-impacted ecosystems in California. *Journal of Environmental Management* 91: 2404–2423.

Finks, S. S., Weihe, C., Kimball, S., Allison, S. D., Martiny, A. C., Treseder, K. K., & Martiny, J. B. (2021). Microbial community response to a decade of simulated global changes depends on the plant community. *Elementa: Science of the Anthropocene*, *9*(1).

Freudenberger DO, Fish BE, Keeley JE (1987) Distribution and stability of grasslands in the Los Angeles basin. Bull South Calif Acad Sci 86:13–26

Gaertner, M., A. Den Breeyen, C. Hui,and D. M. Richardson. 2009. Impacts of alien plant invasions on species richness in Mediterranean-type ecosystems: a meta-analysis. *Progress in Physical Geography* 33: 319–338.

Gea-Izquierdo, G., Gennet, S., & Bartolome, J. W. (2007). Assessing plant-nutrient relationships in highly invaded Californian grasslands using non-normal probability distributions. *Applied vegetation science*, *10*(3), 343-350.

Gray, J. T., & Schlesinger, W. H. (1981). Biomass, production, and litterfall in the coastal sage scrub of southern California. *American Journal of Botany*, *68*(1), 24-33.

Griffin, D., & Anchukaitis, K. J. (2014). How unusual is the 2012–2014 California drought?. *Geophysical Research Letters*, *41*(24), 9017-9023.

Harrison, A.T., Small, E. and Mooney, H.A. (1971), Drought Relationships and Distribution of Two Mediterranean-Climate California Plant Communities. Ecology, 52: 869-875.

Holland VL, Keil DJ (1995) California vegetation. Kendall/Hunt, Dubuque, Iowa

Jiménez MA, Jaksic FM, Armesto JJ, Gaxiola A, Meserve PL, Kelt DA, Gutiérrez JR (2011) Extreme climatic events change the dynamics and invasibility of semi-arid annual plant communities. Ecol Lett 14:1227–1235.

Jones C (2000) Occurrence of extreme precipitation events in California and relationships with the Madden-Julian oscillation. J Climate 13:3576–3587.

Keeley, J.E. (1986) Resilience of Mediterranean shrub communities to fires. *Resilience in Mediterranean-Type Ecosystems* (eds B. Dell, A.J.M. Hopkins & B.B. Lamont), pp. 95–112. Dr W. Junk Publishers, Dordrecht, the Netherlands.

Khalili, B., Oladele A. Ogunseitan, Michael L. Goulden, Steven D. Allison, Interactive effects of precipitation manipulation and nitrogen addition on soil properties in California grassland

and shrubland,Applied Soil Ecology, Volume 107, 2016 , Pages 144-153, ISSN 0929-1393,https://doi.org/10.1016/j.apsoil.2016.05.018.

Kimball, S., Goulden, M.L., Suding, K.N. and Parker, S. (2014), Altered water and nitrogen input shifts succession in a southern California coastal sage community. Ecological Applications, 24: 1390-1404.

McCaull, J. 1994. The Natural Community Conservation Planning Program and the coastal sage scrub ecosystem of southern California. Pages 281 – 292 in R. E. Grumbine, editor. *Environmental policy and biodiversity*. Island Press, Washington, D.C.

Minasny, B., Malone, B. P., McBratney, A. B., Angers, D. A., Arrouays, D., Chambers, A., ... & Winowiecki, L. (2017). Soil carbon 4 per mille. *Geoderma*, *292*, 59-86.

Minnich, R. A., & Dezzani, R. J. (1998). Historical decline of coastal sage scrub in the Riverside-Perris Plain, California. *Western Birds*, *29*(4), 366-391.

Noss, R.F.; Laroei, E.T.; Scott, J.M. 1995. Endangered ecosystems of the United States: A preliminary assessment of loss and degradation. Biological Report 28. US National Biological Service, Washington, DC. Available at: http://biology.usgs.gov/pubs/ecosys.htm

O'Leary, J., Murphy, D. & Brussard, P. (1992) *The Coastal Sage Scrub Community Conservation Planning Region*. Natural Community Conservation Planning/Coastal Sage Scrub Special Report No. 2. California Environmental Trust, San Francisco, CA.

Parolari, A.J., M.L. Goulden, R.L. Bras (2012) Fertilization effects on the ecohydrology of a southern California annual grassland, Geophys. Res. Lett., 39, p. L08405

Parolari, A., Goulden, M., & Bras, R. (2015). Ecohydrological controls on grass and shrub above-ground net primary productivity in a seasonally dry climate. ECOHYDROLOGY, 8(8), 1572-1583.

Pasquini, S. (2008). Vegetation responses to anthropogenic nitrogen deposition and nitrogen fertilization in chaparral and coastal sage scrub of Southern California. Master's Thesis, California State University San Marcos.

Rundel PW (2007) Sage Scrub. In: Barbour MG, Keeler-Wolf T, Schoenherr AA, editors. Terrestrial vegetation of California. 3rd ed. Berkeley: University of California Press. pp. 208–228.

Schmidt, M. W., Torn, M. S., Abiven, S., Dittmar, T., Guggenberger, G., Janssens, I. A., ... & Trumbore, S. E. (2011). Persistence of soil organic matter as an ecosystem property. *Nature*, *478*(7367), 49-56.

Seabloom EW, Harpole WS, Reichmann OJ, Tilman D (2003) Invasion, competitive dominance, and resource use by exotic and native California grassland species. Proc Natl Acad Sci 100:13384–13389

Seager, R., & Vecchi, G. A. (2010). Greenhouse warming and the 21st century hydroclimate of southwestern North America. *Proceedings of the National Academy of Sciences*, *107*(50), 21277-21282.

Sollins, P., Homann, P., & Caldwell, B. A. (1996). Stabilization and destabilization of soil organic matter: mechanisms and controls. *Geoderma*, *74*(1-2), 65-105.

Stylinski, C. D.,and E. B. Allen. 1999. Lack of native species recovery following severe exotic disturbance in southern Californian shrublands. *Journal of Applied Ecology* 36: 544–554.

Talluto, M.V., Suding, K.N. Historical change in coastal sage scrub in southern California, USA in relation to fire frequency and air pollution. *Landscape Ecol* **23,** 803–815 (2008).

Tibor, D. (2001) *Inventory of Rare and Endangered Plants of California*, 6th edn. California Native Plant Society, Sacramento, CA.

Vila, M., J. A. Burriel, J. Pino, J. Chamizo, E. Llach, M. Porterias,and M. Vives. 2003. Association between *Opuntia* species invasion and changes in land-cover in the Mediterranean region. *Global Change Biology* 9: 1234–1239.

Westman, W. E., & O'Leary, J. F. (1986). Measures of resilience: the response of coastal sage scrub to fire. *Vegetatio*, *65*(3), 179-189.

Wolkovich, E. M., Lipson, D. A., Virginia, R. A., Cottingham, K. L., & Bolger, D. T. (2010). Grass invasion causes rapid increases in ecosystem carbon and nitrogen storage in a semiarid shrubland. *Global Change Biology*, *16*(4), 1351-1365.

Wood YA, Meixner T, Shouse PJ et al (2006) Altered ecohydrologic response drives native shrub loss under conditions of elevated nitrogen deposition. J Environ Qual 35:76–92

Xu, X., Shi, Z., Li, D., Rey, A., Ruan, H., Craine, J. M., ... & Luo, Y. (2016). Soil properties control decomposition of soil organic carbon: Results from data-assimilation analysis. *Geoderma*, *262*, 235-242.

Zink, T.A., Allen, M.F. (1998), The Effects of Organic Amendments on the Restoration of a Disturbed Coastal Sage Scrub Habitat. Restoration Ecology, 6: 52-58.

Chapter 4.

Do recent NDVI trends demonstrate boreal forest decline in Alaska?

As published in:

Fiore, N. M., Goulden, M. L., Czimczik, C. I., Pedron, S. A., & Tayo, M. A. (2020). Do recent NDVI trends demonstrate boreal forest decline in Alaska?. *Environmental Research Letters*, *15*(9), 095007.

4.1 Abstract

Remote sensing analyses of boreal forest regions have found widespread decreasing or increasing trends in normalized difference vegetation index (NDVI). Initially, these trends were attributed to climate change induced shifts in primary productivity. It is emerging, however, that fire disturbance and subsequent succession also strongly impact the optical properties of boreal forests. Here we use NDVI time series data from Landsat (1999–2018) paired with surveys of 102 forest stands with known recent fire history to investigate the relationship between NDVI and forest structure during succession. We found that NDVI varies systematically with stand age as a result of successional changes in forest structure and composition and that the proportion of deciduous (broad-leaved) trees in the upper canopy is a better predictor of NDVI than leaf area index. Recent fire disturbance led to strong NDVI decreases and early post-fire recovery of herbaceous and deciduous vegetation to strong NDVI increases. The mid-succession transition from deciduous to evergreen (needle-leaved) stands led to weak NDVI decreases, while mid-to-late succession thinning of evergreen canopies led to weak NDVI increases. Thus, both increasing and decreasing NDVI stands occur naturally across the landscape, and do not necessarily reflect a large-scale shift in boreal forest productivity.

4.2 Introduction

Boreal forests account for nearly one third of global forest area and store ~30% of the total terrestrial ecosystem carbon pool, but climate change, increased fire, and human disturbance may be altering forest dynamics and productivity (Kasischke et al., 1995; Pan et al., 2011; Ma et al., 2012; Bradshaw and Warkentin, 2015). Remote sensing provides a valuable tool for studying the composition and productivity of this large and often inaccessible region, and many studies have utilized satellite-derived measurements of normalized difference vegetation index (NDVI) to infer landscape-scale productivity. Time series are used to calculate NDVI trends over time, with NDVI decreases interpreted as 'browning' and NDVI increases interpreted as 'greening' (Goetz et al., 2005). Previous studies have reported various regional trends, with large spatial and intensity differences between datasets (e.g. GIMMS vs Landsat) and methodologies (Alcaraz-Segura et al., 2010; de Jong et al., 2011; Forkel et al., 2013; Guay et al., 2014).

Previous studies comparing NDVI trends across datasets have found conflicting results, with some showing NDVI increases and others decreases for the same location (Alcaraz-Segura et al., 2010). One source of discrepancy in NDVI analyses lies in the resolution of the dataset, which ranges from 8 km resolution for the Global Inventory Monitoring and Modeling Studies (GIMMS) Advanced Very High-Resolution Radiometer (AVHRR) data to 30 m for Landsat data. Recent work has emphasized finer resolution datasets like Landsat to better diagnose the drivers of changing NDVI (Ju and Masek, 2016; Sulla-Menashe et al., 2018).

A second issue involves the interpretation of NDVI itself. Many studies have tied NDVI to field measurements of biophysical properties of vegetation and found positive correlations with vegetation cover, leaf area index (LAI), biomass, vegetation health, and chlorophyll concentration

(Carlson and Ripley, 1997; McMillan and Goulden, 2008; Yang et al., 2017). However, these biophysical properties are not fully independent, which challenges efforts to interpret recent NDVI trends in terms of changes in actual ecological or biophysical properties. Furthermore, relationships between biophysical properties and NDVI may not hold throughout the whole life history of a forest stand. For example, NDVI increases linearly with LAI for stands with low LAI before saturating at high LAI (Carlson et al., 1990; Turner et al., 1999). These ambiguities underscore the need for systematic field observations to better interpret observed changes in remotely sensed vegetation indices.

We made field observations of vegetation structure and composition at over 100 forest stands of varying age in interior Alaska to investigate the relationship between recent NDVI trends and forest structure and composition. Locations were selected based on fire history and the 1999–2018 Landsat NDVI trend to sample four groups: (1) Stands that burned after 2005; (2) Stands that burned during 1980 and 2005; (3) Stands with no burn reported since 1980 and a decreasing NDVI; and (4) Stands with no burn reported since 1980 and an increasing NDVI. This collection of stands allowed us to explore four questions: (1) How are changes in forest structure and composition in recently burned stands associated with NDVI decreases? (2) How are changes in forest structure and composition in young stands associated with NDVI increases? (3) In the absence of recent fire, how are NDVI decreases in mid-to-late successional forests related to forest structure and composition? (4) In the absence of recent fire, how are NDVI increases in mid-to-late successional forests related to forest structure and composition?

4.3 Methods

Fire history

We used the 1940–2018 Alaskan fire perimeter database produced by the Alaska Fire Service (AFS) and acquired from the Alaska Interagency Coordination Center (https://fire.ak.blm.gov/incinfo/aklgfire.php) to identify sample locations. We subsequently determined the actual age of each stand with tree cores, so errors in the fire perimeter database and the lack of fire history information before 1940 would not affect our analysis.

NDVI extraction and temporal trend analysis

June-August Collection 1, Level 1 Landsat 5, 7, and 8 Surface Reflectance and Brightness Temperature images with less than 30% cloud cover for WRS2 Paths 66–72 and rows 14–16 were downloaded from the USGS (https://espa.cr.usgs.gov; 658 images total; 604 images after 1998) after reprojection at 0.0002695° resolution (30 m latitude, variable longitude). The images were masked for snow, cloud and cloud shadow, and NDVI was calculated, homogenized across instruments and the summer median calculated (see details in Goulden and Bales, 2019). Images were not masked for standing water. There was some residual effect of the Landsat 7 Scan Line Corrector (SLC) failure despite masking, presumably due to systematic alignment of gaps and resulting differences in scene availability. Subsequent analyses focused on 1999–2018 due to large gaps in the earlier record with the lack of a consistent downlink station in Alaska. Simple linear regressions were calculated from the resulting NDVI summer medians over the 20 years time period. Trends with a significant non-zero slope were calculated using a two-tailed t-test, at $p \leq 0.1$ (slopes were considered significant for $\alpha \leq 0.05$ or ≥ 0.95).

Field sites

We surveyed 102 forest stands across interior Alaska, spanning a distance of over 425 km (Figure 4.1) in August 2017 and 2018. The sites were selected before visiting the field to include locations with and without a fire since 1940. Recently burned sites were selected to span a range of years since fire, while sites without a recent fire were selected to include a range of Landsat NDVI trends.

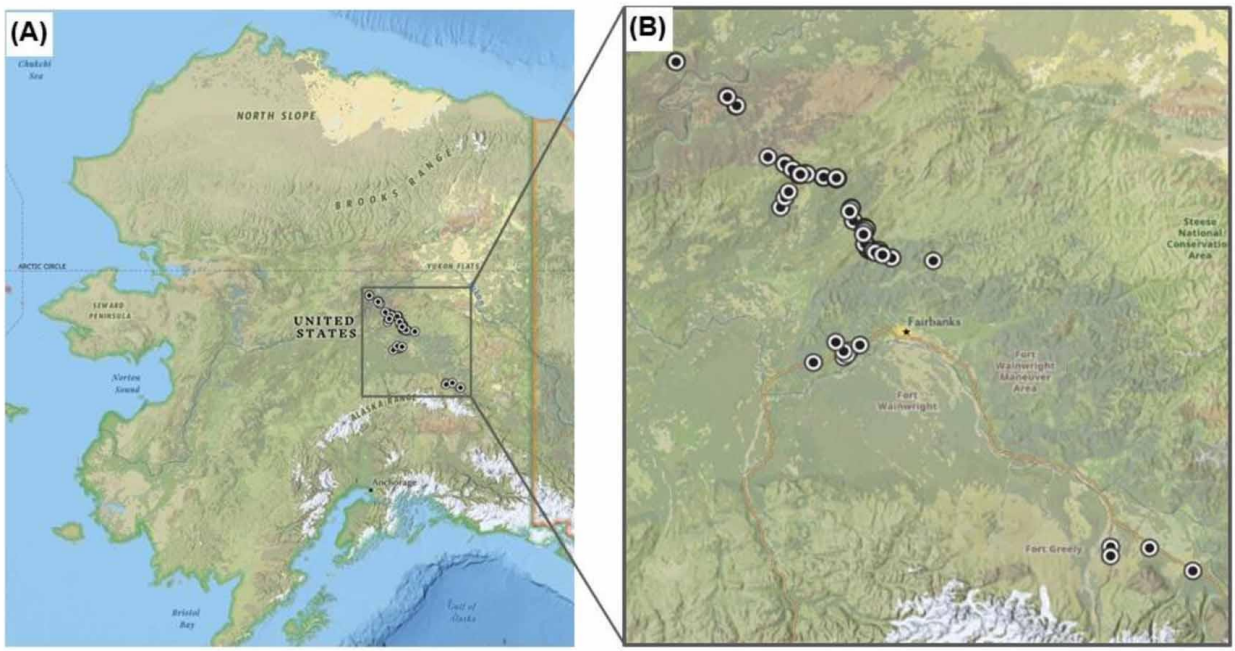

Figure 4.1. Map of A.) Alaska and B.) locations of boreal forest stands around Fairbanks where forest structure and composition were measured and compared to remotely-sensed NDVI trends (From ArcGIS; Sources: Esri, HERE, Garmin, Intermap, INCREMENT P, GEBCO, USGS, FAO, NPS, NRCAN, GeoBase, IGN, Kadaster NL, National Geographic, UNEP-WCMC, NASA, ESA, GEBCO, NOAA, Ordnance Survey, Esri Japan, METI, Esri China (Hong Kong), © OpenStreetMap contributors, GIS User Community).

Sites were further screened to avoid large topographic and land use gradients and to allow efficient access. Two perpendicular 60 m transects were established at each site, and stand

characteristics were measured at 10 m intervals along each transect. Measurements included canopy cover, percent species composition of upper and lower canopies (measured as proportional cover of species over total area on interval), average height of upper and lower canopies, ground cover, standing and downed deciduous stems, and standing and downed evergreen stems. Any evidence of disturbance (fire, permafrost thaw, beetle damage, logging, or other human impacts) was noted. Fraction deciduous was subsequently calculated from the proportion of deciduous cover in the upper canopy over the total canopy coverage.

LAI (leaf area index) data were collected at each site using LAI-2000 plant canopy analyzer (LI-COR). Eight LAI-2000 measurements were taken under the canopy in each 30 m interval along the 60 m perpendicular transects and corresponding above canopy measurements were taken in the nearest canopy clearing. The measurements were then processed with the internal LI-COR LAI software to provide four estimations of LAI per site. The LAI-2000 is known to underestimate LAI in coniferous stands, so species specific corrections for black spruce (*Picea mariana* (Mill.) B.S.P.) were applied to black spruce site data (Chen 1996; Law et al., 2008). Corrections for white spruce (*Picea glauca* (Moench) Voss) are not available, and these stands were frequently mixed with deciduous species; we consequently were unable to correct for clumping in the white spruce stands and note that LAI may be underestimated at these sites. The mean LAI was then calculated from the four estimations and used as the site level LAI.

To estimate tree age of each site, multiple tree cores were collected from representative trees of each species in the upper canopy (2–4 trees per species) with 4.3 mm outer diameter increment borers (Haglöf). Tree cores were mounted, sanded manually, and rings were counted using Lignovision software (Rinntech). The average tree age was subsequently determined by

taking the mean ring count of cores analyzed. For recently burned and early fire recovery sites the site age was determined from the year of fire and confirmed by tree cores when possible.

4.4 Results

Composition and structure of successional stages

The sites visited were subsequently sorted into five successional stages based on stand age and majority (>50%) species composition of the upper canopy: (1) Recently burned (fire after 2005; ≤13 years since fire), (2) Early fire recovery (burned between 1980–2005; 13–38 years since fire), (3) Mid-to-late successional, deciduous dominated stand, (4) Mid-to-late successional, white spruce dominated stand, and (5) Mid-to-late successional, black spruce dominated stand.

Each successional stage had a distinct forest structure, and a characteristic NDVI trend (Figure 4.2). Recently burned stands (age 0–13 years) had charred, dead trees with occasional live, evergreen trees in the upper canopy that survived the fire, and deciduous saplings in the lower canopy (Figure 4.3). Herbaceous plants, moss, and charred material covered most of the ground. Early fire recovery stands (age 13–38 years) had upper canopies of evergreen trees that had survived fire, along with deciduous species such as paper birch (*Betula papyrifera* Marshall) and quaking aspen (*Populus tremuloides* Michx.), and lower canopies of birch and aspen, and mostly herbaceous ground cover (Figure 4.3). Standing and fallen dead trees from the fire were still visible. Mid-to-late successional deciduous stands (age 30–180 years) had dense upper canopies of birch and aspen, and lower canopies of birch, aspen, and alder (*Alnus sps*.), with progressively more white spruce or black spruce in older stands (Figure 4.3). The ground cover of deciduous stands consisted of bare ground and litter, herbaceous plants and small percentages of moss. Mid-to-late successional white spruce stands (age 50–200 years) often had multiple generations of white

spruce in the upper canopy, with varying percentages of deciduous species in the upper canopy, and lower canopies of white spruce with dense thickets of alder (Figure 4.3). Mid-to-late successional black spruce (age 30–200 years) had sparse black spruce in both the upper and lower canopies, and occasionally small percentages of birch and willow (*Salix* sp.) in the upper and lower canopies. Thick layers of moss, lichen, and herbaceous plants covered most of the ground in mid-to-late successional black spruce stands (Figure 4.3).

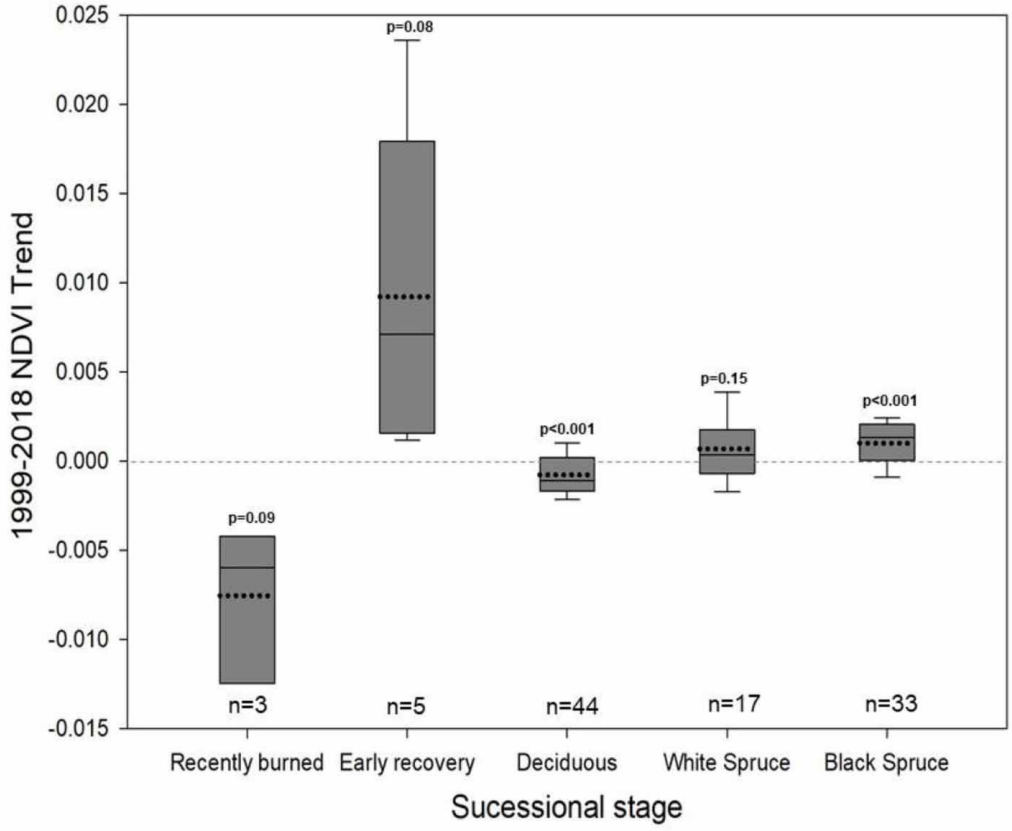

Figure 4.2. Boxplots of all 1999–2018 NDVI trends (NDVI units/year) for each successional stage. Dotted line indicates mean, solid line indicates median. Sample size (number of sites visited) is shown above each successional stage label, and p-value calculated using a two-tailed, one sample t-test on all trends for each group is shown above each boxplot. Null hypothesis is that the mean trend for each group is '0'.

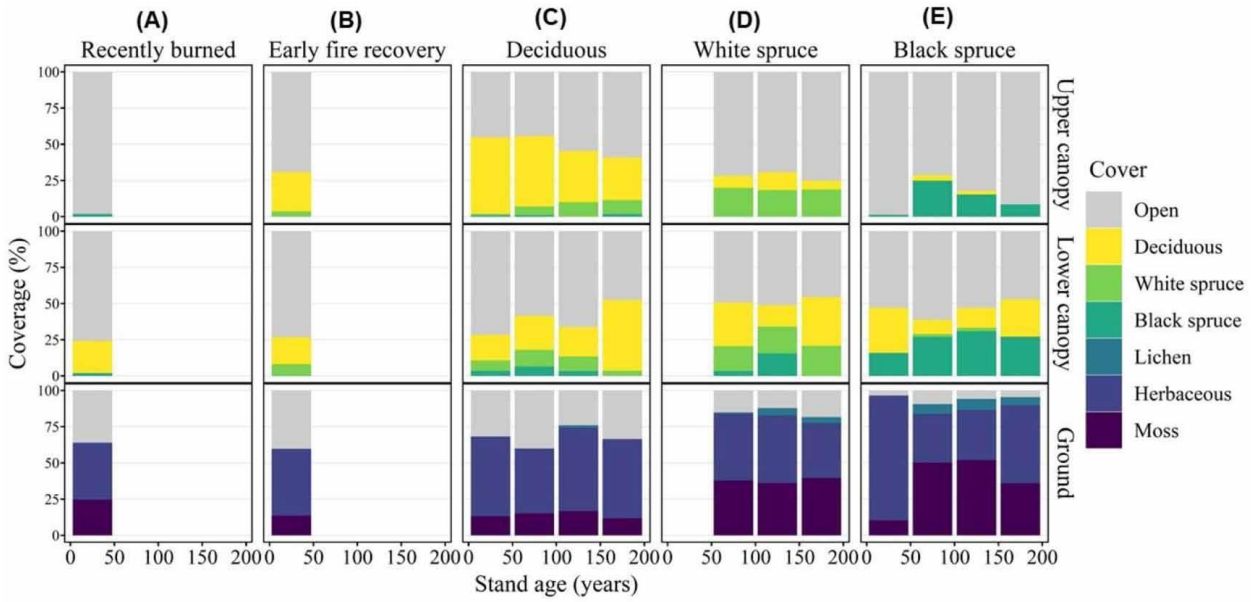

Figure 4.3. Chronosequences of composition (based on percent cover) of upper and lower canopies, and ground cover binned by stand age in 50-year intervals for each successional stage. Calculated from field data collected in 2017–2018. A.) Recently burned forest composition (stand age 0–13 years); B.) Early fire recovery forest composition (stand age 13–38 years); C.) Mid-to-late successional deciduous dominated forest composition (stand age 30–180 years); D.) Mid-to-late successional white spruce dominated forest composition (stand age 50–200 years); E.) Mid-to-late successional black spruce dominated forest composition (stand age 30–200 years).

NDVI trends across the landscape

There was a visible mosaic of increasing and decreasing NDVI trends across interior Alaska, which was clearly linked with recent fire history (Figure 4.4). Burn scars from recent decades show consistent behavior in NDVI trends, with trend perimeters typically matching fire perimeters. Timing of fire largely controlled NDVI trend direction and intensity, with recent burns (2018–2005) showing strong NDVI decreases and burns from 2005–1980 showing NDVI increases (Figures 4.4). Trend significance inside burn scar perimeters was variable, with some pixels showing significant trends (p-value < 0.1), and others insignificant within the same burn scar (Figure 4.4B).

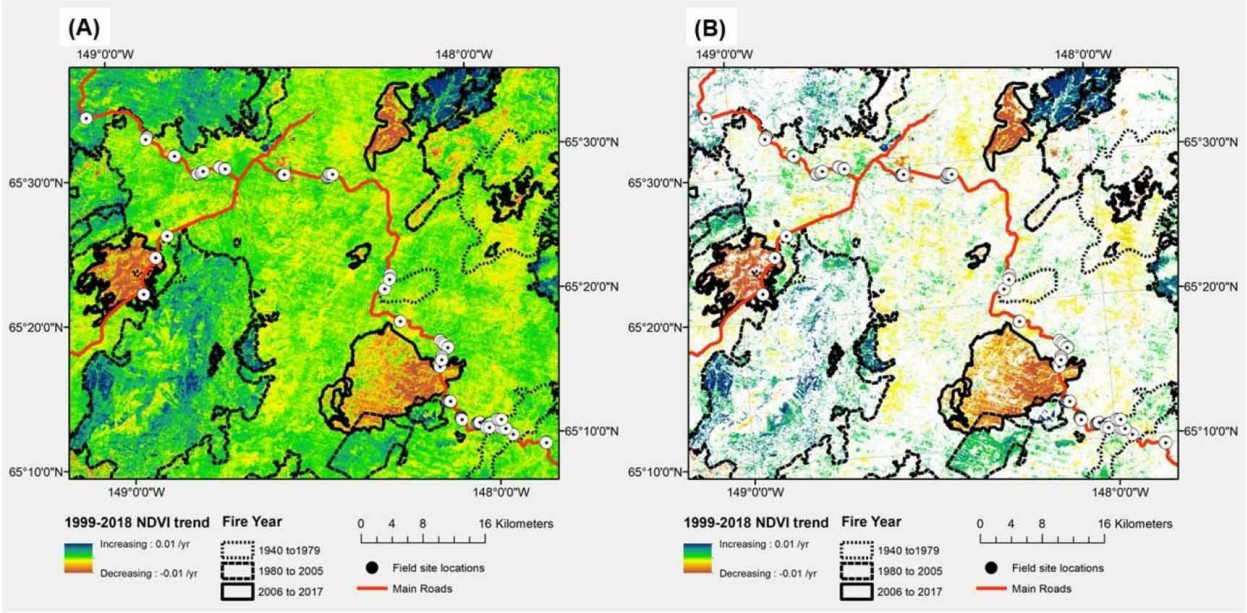

Figure 4.4. Fire history polygons overlaid on map of NDVI linear regression trends from 1999–2018 (NDVI units per year) across interior Alaska. A.) NDVI trend from 1999–2018 for each pixel. B.) Significant NDVI trends from 1999–2018, with insignificant trends shown as white. Trend significance in B.) was tested using a two-tailed t-test on the linear regression trend of each pixel; all significant pixel trends (p-value < 0.1) are shown in color based on the magnitude of the trend, and all insignificant pixel trends (p-value > 0.1) are shown in white.

There was heterogeneity in NDVI trends in the absence of recent fires, with some undisturbed patches showing increasing NDVI and others showing decreasing NDVI. These undisturbed patches often showed smaller magnitude trends than areas with reported fires, though 17.2% of these trends were significant (p-value < 0.1) (Figure 4.4B). Moreover, the unburned locations with significant trends were clustered in relatively homogenous patches (Figures 4.4B), and were not intermixed with pixels of opposite slope as would be expected with a random distribution, implying that NDVI trends in the absence of recent fire may reflect ecological variation.

Successional effects on NDVI

Our data allowed us to create a 200 years long chronosequence of the boreal forest NDVI successional trajectory (Figure 4.5), and to calculate the resulting 20 years chronosequence of NDVI trends related to recent fires (since 1940) (Figure 4.6). Stands with recent fire displayed large ranges in NDVI due to the rapid changes in forest structure and composition following fire, but overall had the lowest average NDVIs (Figure 4.5A). Fire disturbance caused a sharp drop in NDVI due to the loss of vegetation, followed by rapid recovery of herbaceous and deciduous vegetation leading to strong NDVI increases (Figures 4.3 and 4.5B). NDVI continued to increase until around 30 years since fire (Figure 4.5A), at which point many stands displayed maximum fraction deciduous in the upper canopy (Figure 4.3). The immediate effect of fire and subsequent recovery were large drivers of NDVI change in stands <30 years old (Figures 4.5B and 4.6).

After stands reached 30 years of age, NDVI typically stabilized and displayed more gradual changes. Mid-to-late successional deciduous stands collectively had the highest summer median NDVI, followed by white spruce, then black spruce stands (Figure 4.5A). With increasing age, deciduous stands exhibited weak NDVI decreases and black spruce stands of all ages showed weak NDVI increases (Figures 4.2 and 4.5B). White spruce stands displayed both decreasing and increasing trends, with younger white spruce stands typically showing decreases, and older white spruce stands showing increases (Figures 4.2 and 4.5B).

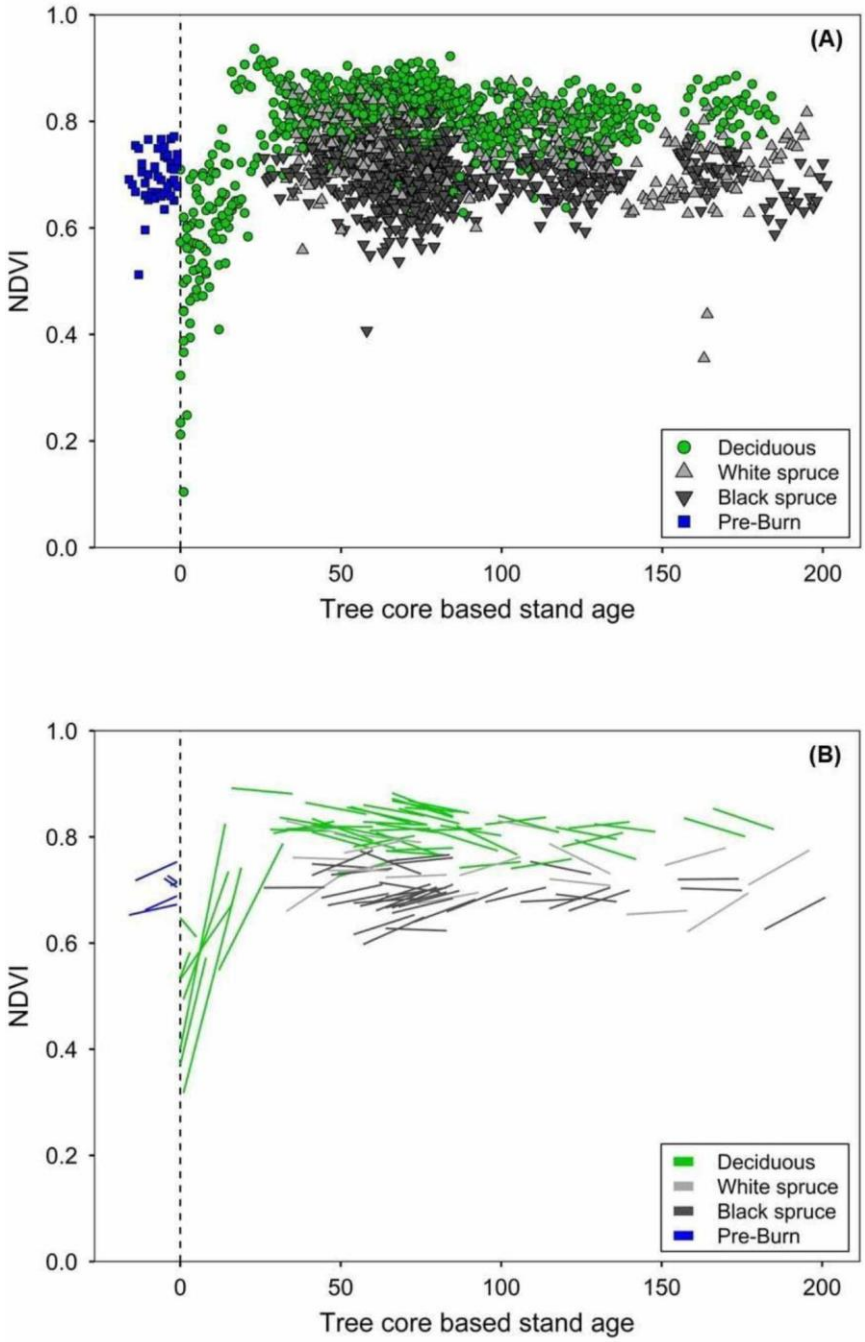

Figure 4.5. Chronosequences of NDVI of all sites visited, separated by dominant vegetation in the upper canopy during 2017–2018. A.) Annual summer median NDVI from 1999–2018 for each site visited. B.) NDVI trend for each site during 1999–2018. Tree core-based stand age of '0' represents the year of fire, with 'Pre-Burn' assigned as negative ages, or years before fire.

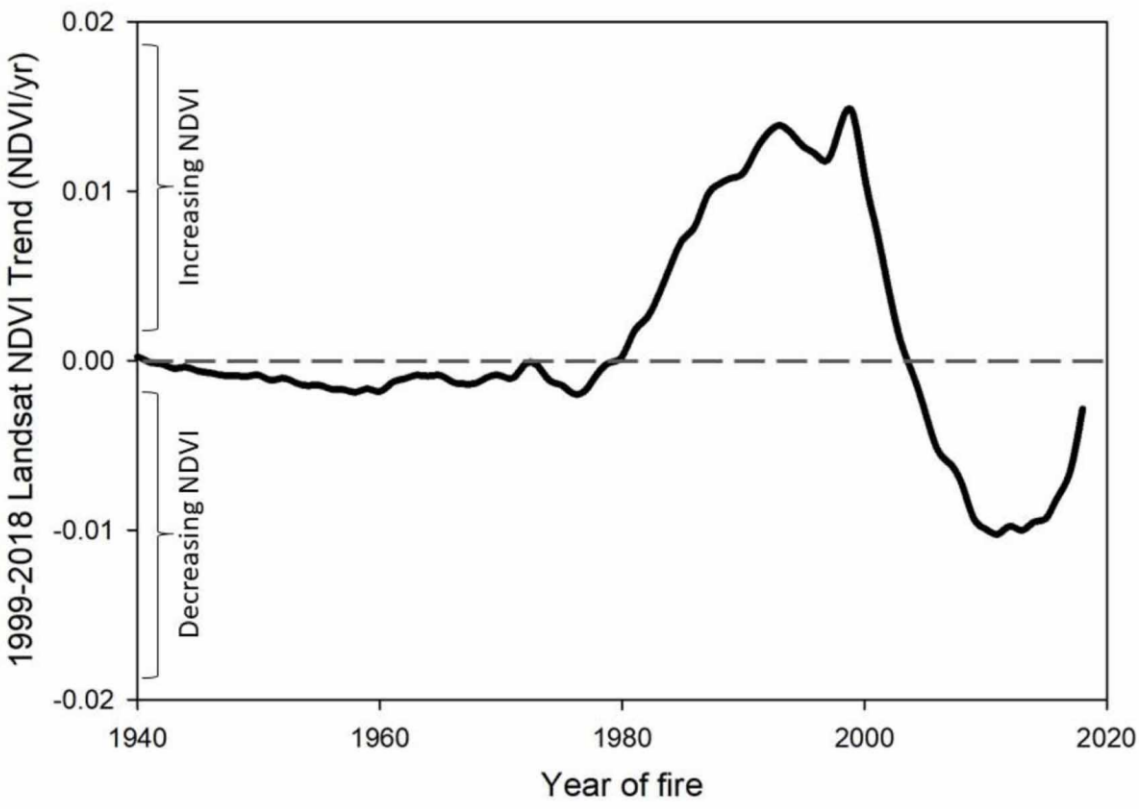

Figure 4.6. NDVI trend during 1999–2018 as a function of year of fire. NDVI trend was calculated from the slope of a floating 20 years window on the chronosequence of all NDVI observations for all stand types with a reported fire since 1940.

Ecological effects on NDVI

The relationship between successional stage and NDVI can be explored further by examining the relationships between fraction deciduous in the upper canopy and NDVI, and LAI and NDVI. We found that NDVI was positively correlated with fraction deciduous in the upper canopy (r^2= 0.63) and with LAI (r^2= 0.15) (Figure 4.7). Deciduous stands by definition had the highest fraction deciduous and highest NDVI. These stands showed marked variation in LAI, which was correlated with differences in NDVI, especially in sparsely vegetated, recent burns. Compared to deciduous stands, white spruce stands had a smaller fraction deciduous, a smaller

range in LAI, and lower NDVI. Here, upper canopies typically consisted of a mixture of white spruce and deciduous species and an increasing fraction deciduous generally increased NDVI (Figures 4.3 and 4.76A). Black spruce stands had the lowest NDVI, a relatively small range in LAI, and were less likely to have deciduous species in the upper canopy. Overall, fraction deciduous in the upper canopy was a stronger predictor of NDVI than LAI.

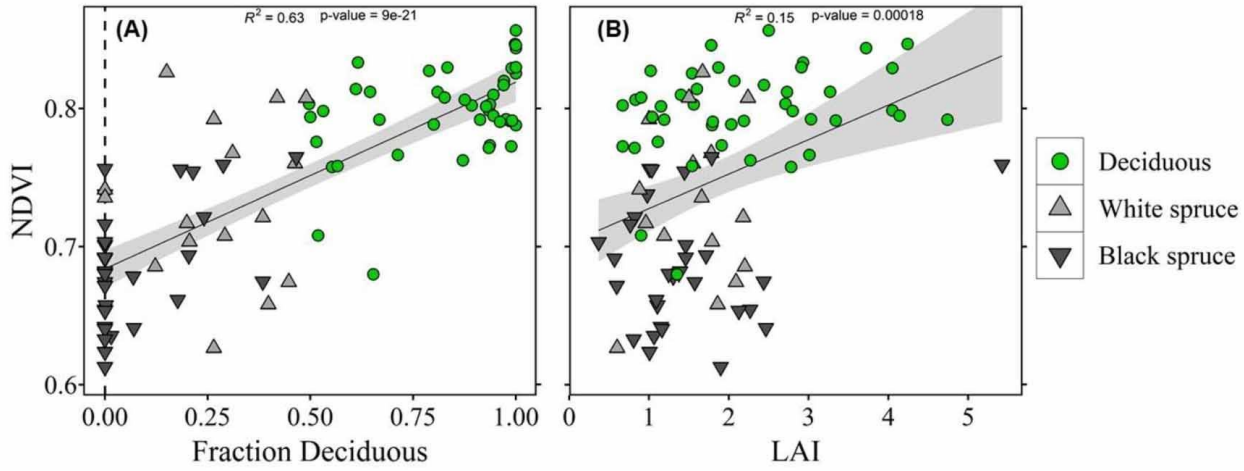

Figure 4.7. Relationships between fraction deciduous and NDVI, and LAI and NDVI of boreal forest stands in Interior Alaska, USA. A.) Relationship between fraction deciduous of the upper canopy, calculated from the proportion of deciduous cover over total canopy cover and NDVI for year sampled; B.) Relationship between mean, site level LAI (taken with LAI-2000) and NDVI for year sampled. Recently burned sites (<13 years since fire) are not shown due to their lack of upper canopy.

4.5 Discussion

The central concept addressed in this study is how changes in the biophysical properties of forests following fire and subsequent succession impact NDVI. Our results indicate that fire was the main driver of large changes in NDVI in our sites. Fires after 2005 were associated with large decreases in NDVI due to vegetation loss from fire, and fires between 1980 and 2005 with large increases in NDVI due to post fire recovery of deciduous vegetation (Figures 4.2, 4.4 and 4.6) (see

also Randerson et al., 2006; Alcaraz-Segura et al., 2010; Ju and Masek, 2016). The NDVI increases from fire recovery last for roughly 30 years post-fire, at which point many stands displayed maximum fraction deciduous (Figures 4.3, 4.5A and 4.7). This finding is supported by (Beck and Goetz, 2011) who also found that high NDVI coincided with high deciduous coverage around 20–40 years post-fire, and by (Amiro et al., 2006) who found high albedo around 30 years post-fire that was linked to high deciduous coverage.

After this peak in NDVI and deciduous cover, mid-succession changes in forest structure and composition led to weak decreases in NDVI in deciduous stands (Figures 4.2 and 4.5B). We believe the ongoing replacement of high-NDVI deciduous, broad-leaved trees with lower-NDVI evergreen, needle-leaved trees explains this trend, as evidenced by the changes seen in forest composition (Figure 4.3) and the relationship between fraction deciduous and NDVI (Figure 4.7A). Our results confirm that NDVI saturates at high LAI (Figure 4.7B) (Carlson et al., 1990; Gong et al., 1995; Turner et al., 1999), and that fraction deciduous in the upper canopy is a better predictor of NDVI than LAI in boreal forests.

Our data also indicate a mid-to-late succession NDVI increase, especially evident in black spruce stands and older white spruce stands (Figures 4.2 and 4.5B). We believe this increasing trend in NDVI is due to the natural self-thinning and, or paludification of evergreen forests over time that reveals understories with higher NDVI, consisting of deciduous shrubs, grasses, and/or mosses (Figure 4.3). These results are consistent with previous work showing that NDVI trends are related to cover type and that forests with sparse tree cover often show increasing NDVI trends (Bunn and Goetz, 2006; Miles and Esau, 2016). As such, our work further supports the conclusion that the understory of sparse forests plays a large role in remotely sensed NDVI and that increasing NDVI is a poor proxy of tree productivity (Caetano and Pereira, 1996).

Many previous studies have documented widespread NDVI decreases across boreal forests, which were hypothesized to reflect climate change-induced drought stress (Goetz et al., 2005; Bunn and Goetz, 2006; Parent and Verbyla, 2010) and later linked to changes in productivity via tree ring width analyses (Beck et al., 2011; Bunn et al., 2013). However, our study demonstrates that changes in NDVI also signal changes in forest species composition and structure that are not directly related to productivity and/or vegetation health. While the use of satellite-derived vegetation indices such as NDVI to analyze vegetation dynamics remotely has clear advantages, one evident drawback lies in the difficulty of directly ascribing changes in indices to the biophysical or ecological properties of forests and their understories on the ground.

One limitation of our study is that our geographic location did not cross any ecotones where climate change impacts are more likely to affect productivity (Goetz et al., 2005; Andreu-Hayles et al., 2011; Sulla-Menashe et al., 2018). However, Landsat's 30 m resolution allowed us to better link NDVI to *in situ* forest properties. Our results indicate that NDVI varies systematically with stand age and successional stage, and that both fire and natural succession lead to composition and structure changes that cause changes in NDVI, and do not necessarily reflect climate change induced changes in tree productivity.

4.6 Conclusion

Our study linking surveys of forests with remotely-sensed NDVI demonstrates how boreal forest fire and succession impact NDVI, and that fraction deciduous in the upper canopy is a better predictor of NDVI than LAI in boreal forests. We conclude that the immediate and legacy effects of fire are strong drivers of changes in boreal NDVI, and that forest patches with both increasing and decreasing NDVI occur naturally across the landscape, and do not unambiguously indicate

large-scale changes in boreal tree productivity. While the response of forests to climate change remains unclear, our results underscore the need to deconvolve the legacy effect of disturbance and recovery when diagnosing recent trends in forest structure and function.

4.7 Acknowledgements

This work was funded by NASA ABoVE #NNX15AU16A (to M.L.G. and C.I.C.) and UCI's Undergraduate Research Opportunity Program (to M.A.T.). This work was supported by the Ridge to Reef NSF Research Traineeship (DGE-1735040 to N.M.F and S.A.P.). We thank S. Sackett (Fairbanks ABoVE field office) for logistical support during field campaigns. We thank C.D. Elder for his help with data collection in 2017.

4.8 References

Alcaraz-Segura D., Chuvieco E., Epstein H. E., Kasischke E. S. and Trishchenko A. 2010 Debating the greening vs. browning of the North American boreal forest: differences between satellite datasets *Glob. Change Biol.* 16 760–70

Amiro B. et al., 2006 The effect of post-fire stand age on the boreal forest energy balance *Agric. For. Meteorol.* 140 41–50

Ams M. and Goulden M. L. 2008 Age-dependent variation in the biophysical properties of boreal forests *Glob. Biogeochem. Cycles* 22 GB2023

Andreu-Hayles L., D'Arrigo R., Anchukaitis K. J., Beck P. S. A., Frank D. and Goetz S. 2011 Varying boreal forest response to Arctic environmental change at the Firth River, Alaska *Environ. Res. Lett.* 6 045503

Beck P. S. A. and Goetz S. J. 2011 Satellite observations of high northern latitude vegetation productivity changes between 1982 and 2008: ecological variability and regional differences *Environ. Res. Lett.* 6 045501

Beck P. S. A., Juday G. P., Alix C., Barber V. A., Winslow S. E., Sousa E. E., Heiser P., Herriges J. D. and Goetz S. J. 2011 Changes in forest productivity across Alaska consistent with biome shift *Ecol. Lett.* 14 373–9

Bradshaw C. J. A. and Warkentin I. G. 2015 Global estimates of boreal forest carbon stocks and flux *Glob. Planet. Change* 128 24–30

Bunn A. G. and Goetz S. J. 2006 Trends in satellite-observed circumpolar photosynthetic activity from 1982 to 2003: the influence of seasonality, cover type, and vegetation density *Earth Interact.* 10 1–19

Bunn A. G., Hughes M. K., Kirdyanov A. V., Losleben M., Shishov V. V., Berner L. T., Oltchev A. and Vaganov E. A. 2013 Comparing forest measurements from tree rings and a space-based index of vegetation activity in Siberia *Environ. Res. Lett.* 8 035034

Caetano M. R. and Pereira J. M. T. 1996 Effect of the understory on the estimation of coniferous forest leaf area index (LAI) based on remotely sensed data *Proc. SPI* E 2955 63–71

Carlson T. N., Perry E. M. and Schmugge T. J. 1990 Remote estimation of soil moisture availability and fractional vegetation cover for agricultural fields *Agric. For. Meteorol.* 52 45–69

Carlson T. N. and Ripley D. A. 1997 On the relation between NDVI, fractional vegetation cover, and leaf area index *Remote Sens. Environ.* 62 241–52

Chen J. M. 1996 Optically-based methods for measuring seasonal variation of leaf area index in boreal conifer stands *Agric. For. Meteorol.* 80 135–63

de Jong R., de Bruin S., de Wit A., Schaepman M. E. and Dent D. L. 2011 Analysis of monotonic greening and browning trends from global NDVI time-series *Remote Sens. Environ.* 115 692–702

Esri ‘‘‘National Geographic Style Base’’ [basemap]. ‘‘World National Geographic Style Base’’’ www.arcgis.com/home/item.html?id=30e5fe3149c34df1ba922e6f5bbf808f (Accessed: 22

May 2020)

Forkel M., Carvalhais N., Verbesselt J., Mahecha M., Neigh C. and Reichstein M. 2013 Trend change detection in NDVI time series: effects of inter-annual variability and methodology *Remote Sens.* 5 2113–44

Goetz S. J., Bunn A. G., Fiske G. J. and Houghton R. A. 2005 Satellite-observed photosynthetic trends across boreal North America associated with climate and fire disturbance *Proc. Natl Acad. Sci.* 102 13521–5

Gong P., Pu R. and Miller J. R. 1995 Coniferous forest leaf area index estimation along the Oregon transect using compact airborne spectrographic imager data *Photogramm. Eng. Remote Sens.* 61 1107–17

Goulden M. L. and Bales R. C. 2019 California forest die-off linked to multi-year deep soil drying in 2012–2015 drought *Nat. Geosci.* 12 632–7

Guay K. C., Beck P. S. A., Berner L. T., Goetz S. J., Baccini A. and Buermann W. 2014 Vegetation productivity patterns at high northern latitudes: a multi-sensor satellite data assessment *Glob. Change Biol.* 20 3147–58

Ju J. and Masek J. G. 2016 The vegetation greenness trend in Canada and US Alaska from 1984–2012 Landsat data *Remote Sens. Environ.* 176 1–16

Kasischke E. S., Christensen N. L. and Stocks B. J. 1995 Fire, global warming, and the carbon balance of boreal forests *Ecol. Appl.* 5 437–51

Kasischke E. S. et al., 2010 Alaska's changing fire regime—implications for the vulnerability of its boreal forests *Can. J. For. Res.* 40 1313–24

Law B. E., Arkebauer T., Campbell J. L., Chen J., Sun O., Schwartz M., van Ingen C. and Verma S. 2008 *Terrestrial carbon observations: protocols for vegetation sampling and data submission* (Rome, Italy: Food and Agriculture Organization of United Nations)

Ma Z., Peng C., Zhu Q., Chen H., Yu G., Li W., Zhou X., Wang W. and Zhang W. 2012 Regional drought-induced reduction in the biomass carbon sink of Canada's boreal forests *Proc. Natl Acad. Sci. US* A 109 2423–7

Miles V. and Esau I. 2016 Spatial heterogeneity of greening and browning between and within bioclimatic zones in northern West Siberia *Environ. Res. Lett.* 11 115002

Pan Y. et al., 2011 A large and persistent carbon sink in the world's forests *Science* 333 988–93

Parent M. B. and Verbyla D. 2010 The browning of Alaska's boreal forest *Remote Sens.* 2 2729–47

Randerson J. T. et al., 2006 The impact of boreal forest fire on climate warming *Science* 314 1130–2

Sulla-Menashe D., Woodcock C. E. and Friedl M. A. 2018 Canadian boreal forest greening and browning trends: an analysis of biogeographic patterns and the relative roles of disturbance versus climate drivers *Environ. Res. Lett.* 13 014007

Turner D. P., Cohen W. B., Kennedy R. E., Fassnacht K. S. and Briggs J. M. 1999 Relationships between leaf area index and landsat TM spectral vegetation indices across three temperate zone sites *Remote Sens. Environ.* 70 52–68

Yang H., Yang X., Heskel M., Sun S. and Tang J. 2017 Seasonal variations of leaf and canopy properties tracked by ground-based NDVI imagery in a temperate forest *Sci. Rep.* 7 1267

Chapter 5.

Future research directions

The work presented in Chapters 2 and 3 of this dissertation provide novel findings on the belowground properties and processes of a CSS and GL mosaic in Southern California. The work from Chapter 2 highlighted how overlying vegetation type impacts soil properties along the stable boundary at our site. CSS and GL mosaics are commonly found throughout California, and similar shrub- and grassland mosaics are found worldwide. Future research should investigate local CSS and GL mosaics to determine whether our findings of differences in soil properties hold true across other locations, and between other shrub- and grassland mosaics.

The work from Chapter 3 highlighted the sensitivity of CSS to drought, and the cascading effects of vegetation type shifts between CSS and GL on ecosystem properties and processes above- and belowground. As drought conditions are expected to increase in severity and frequency in Southern California, vegetation shifts from CSS to GL will become more common, leading to significant impacts on ecosystem hydrology, carbon balance, and nutrient cycling. Future research should aim to identify thresholds to the CSS to GL vegetation type shift and explore whether vegetation shifts between CSS and GL are reversible in times of greater rainfall. It will also be important to determine if the drought induced shifts in soil properties become a barrier to CSS recovery, triggering a tipping point in which the ecosystem will no longer be able to return to a functioning CSS community. Further investigations should focus on CSS and GL mosaics that are currently experiencing invasion of GL into CSS, or encroachment of CSS into GL to see if soil properties are impacted by the aboveground vegetation type shifts. This work can also be expanded

to shifting boundaries in other shrub- and grassland mosaics and more broadly between shifting vegetation types (grass and shrub, grass and tree, shrub and tree, tree and tundra) that have been documented globally.

Appendix A.

Supplemental Figures

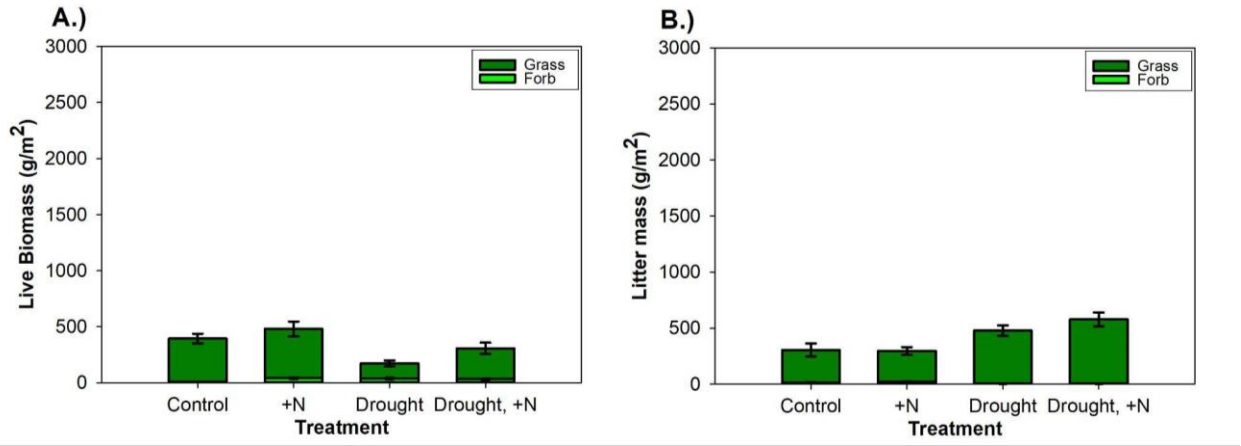

Figure A.1. Live biomass and litter mass pools in Grassland habitat found at the Loma Ridge Global Change Experiment. Error bars indicate standard error of the mean. A.) Live Biomass by plant functional type. B) Litter Mass by type.

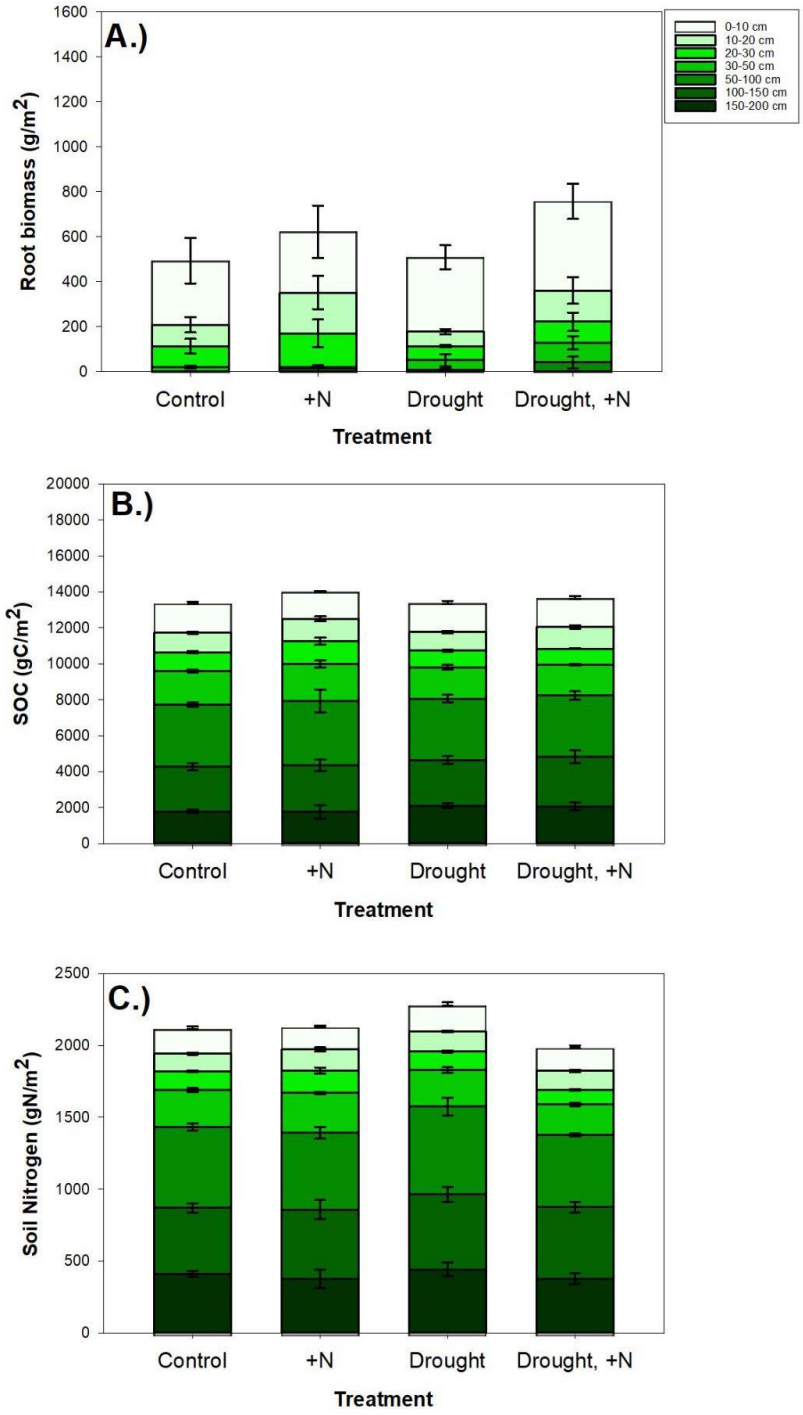

Figure A.2. Root biomass, Soil Organic Carbon, and Soil Nitrogen Stocks in Grassland habitat found at the Loma Ridge Global Change Experiment. Error bars indicate standard error of the mean. A.) Root biomass by depth layer in each treatment. B.) Soil Organic Carbon stocks by depth layer in each treatment. C.) Soil Nitrogen stocks by depth layer in each treatment.

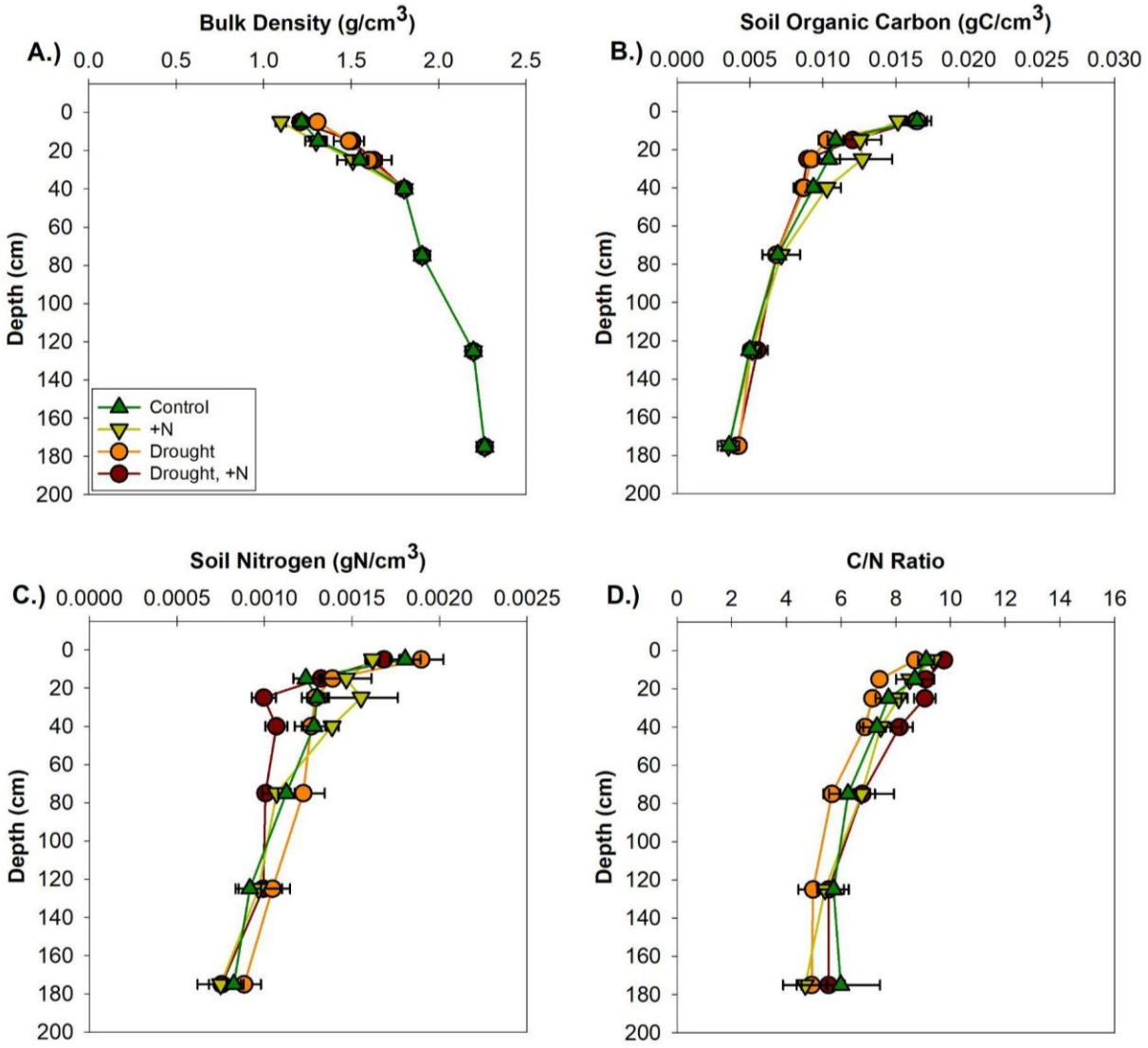

Figure A.3. Soil properties by depth in Grassland habitat found at the Loma Ridge Global Change Experiment. Error bars represent standard error of the mean. A.) Soil bulk density by depth in each treatment. B.) Soil organic carbon by depth in each treatment. C.) Soil nitrogen by depth in each treatment D.) Soil C/N ratio by depth in each treatment.

Appendix B.

Supplemental Tables

Table A.1. Summary of abiotic factors in Grassland (GL) and Coastal Sage Scrub (CSS) vegetation types found along a stable boundary at the Loma Ridge Global Change Experiment.

	Grassland (GL)	Shrubland (CSS)
Mean Elevation (m)	351	356
Minimum Elevation (m)	347	347
Maximum Elevation (m)	360	364
Mean Slope, Aspect	10.2%, NW	10.0%, NW
Soil texture class	Sandy Loam	Sandy Loam
Soil subgroup	*Typic Palexeralfs*	*Typic Palexeralfs*

Table A.2. Summary of P-values from T-tests testing the impact of vegetation type (CSS vs GL) on soil texture by depth. When violations of normality were encountered, Mann- Whitney tests were used, indicated with asterisk (*). P-values in boldface indicate significant differences (P<0.05) between vegetation types.

	0 cm	15 cm	30 cm	45 cm	100 cm	200 cm
Clay	***0.021**	**0.025**	0.185	0.920	***<0.001**	0.154
Silt	***0.006**	**0.007**	0.973	0.453	0.642	0.953
Sand	*0.926	0.804	0.276	0.712	**<0.001**	0.248

Table A.3. Summary of P-values from T-tests testing the impact of vegetation type (CSS vs GL) on aboveground vegetation properties. When violations of normality were encountered, Mann- Whitney tests were used, indicated with asterisk (*). P-values in boldface indicate significant differences (P<0.05) between vegetation types**.**

Live Shrub Biomass	***<0.001**
Live Grass Biomass	***<0.001**
Live Forb Biomass	***0.016**
Shrub Litter Mass	***<0.001**
Grass Litter Mass	***0.010**
Forb Litter Mass	***<0.001**
Total Root Biomass	***0.009**
Total Soil Carbon Stock	**<0.001**
Total Soil Nitrogen Stock	**0.018**

Table A4. Summary of P-values from T-tests testing the impact of vegetation type (CSS vs GL) on belowground properties. When violations of normality were encountered, Mann-Whitney tests were used, indicated with asterisk (*). P-values in boldface indicate significant differences (P<0.05) between vegetation types.

	0-10 cm	10-20 cm	20-30 cm	30-50 cm	50-100 cm	100-150 cm	150-200 cm
Root Biomass	0.336	***0.005**	0.069	***<0.001**	***0.002**	***0.038**	0.105
Root Distribution	**0.025**	0.360	0.166	***0.050**	***0.002**	***0.038**	0.105
Bulk Density	**<0.001**	**<0.001**	**0.005**	0.924	0.461	0.498	0.617
Soil Carbon (gC/kg)	***0.040**	0.160	0.340	0.623	**<0.001**	**0.010**	**0.010**
Soil Carbon (gC/cm3)	***<0.001**	**0.002**	0.101	0.582	**<0.001**	**0.004**	**0.008**
Soil Nitrogen (gN/kg)	**<0.001**	0.219	*0.195	***0.038**	*0.959	*0.130	***0.007**
Soil Nitrogen (gN/cm3)	0.631	0.128	0.966	0.067	0.117	**0.014**	***0.028**
C/N Ratio	**<0.001**	*0.104	**0.030**	0.251	0.543	*0.541	*0.429

Table A.5. Summary of P-values from T-tests testing the impact of vegetation type (CSS vs GL) on belowground distribution of properties. When violations of normality were encountered, Mann- Whitney tests were used, indicated with asterisk (*). P-values in boldface indicate significant differences (P<0.05) between vegetation types.

	0-50 cm	50-100 cm	100-150 cm	150-200 cm
Soil Carbon Distribution	0.988	0.323	0.644	0.445
Soil Nitrogen Distribution	***0.002**	*0.505	0.333	*0.083

Table A.6. Species-specific regression equations relating shrub volume to biomass (g). Total biomass and volume data were natural log transformed to reduce variance. Equations are in the form y = a*x+b, where variable a represents slope and b represents the y-intercept. The general shrub equation was developed by combining all data for all shrubs. Equations marked with asterisk are taken from Pasquini, 2008.

Species	**a**	**b**	**r^2**
*Artemisia californica**	0.8606	-5.7531	0.99
*Eriogonum fasciculatum**	0.7870	-4.9588	0.99
Malosma laurina	0.6990	-3.2400	0.95
*Salvia mellifera**	0.9353	-6.4553	0.99
General shrub*	0.8704	-5.4883	0.97